

**ANKARA UNIVERSITY
GRADUATE SCHOOL OF NATURAL AND APPLIED SCIENCES**

MASTER OF SCIENCE THESIS

**DEVELOPMENT OF 3D PRINTED DISPOSABLE MEDICAL EQUIPMENT TO
COMBAT THE SARS-COV-II PANDEMIC**

Abdullah EYİDOĞAN

DEPARTMENT OF BIOMEDICAL ENGINEERING

**ANKARA
2021**

All rights reserved

ABSTRACT

M.Sc. Thesis

DEVELOPMENT OF 3D PRINTING-BASED DISPOSABLE MEDICAL EQUIPMENT TO COMBAT THE SARS-COV-II PANDEMIC

Abdullah EYİDOĞAN

Ankara University
Graduate School of Natural and Applied Sciences
Department of Biomedical Engineering

Supervisor: Prof. Dr. Pınar YILGÖR HURİ

This thesis study aimed to produce 3D printed medical equipment to combat the SARS-CoV-II pandemic, in order to reduce the risk of transmission between doctor-patient and patient-patient. In this context, it is aimed to design, manufacture and test sterile, disposable tools and personal protection equipment required by the physicians in contact with the patients in the healthcare infrastructures.

Along the thesis, a personal protection equipment (face shields) and a therapeutic equipment (laryngoscope) were 3D printed and tested for their ability to perform as their commercially available counterparts. 3 types of face shields were designed and evaluated for use in the fight against the pandemic. Several designs were prepared for the laryngoscope and their structural stability as well as printability and usability were evaluated with computer simulations and mechanical testing. Moreover, as an important approach to combat the pandemic, two different methods to reduce the aerosol load were designed, produced with 3D printing, and tested in terms of their mechanical properties. A 3D printed guide for aorta stent implantation surgery was created and its ability to mimic natural tissue was tested mechanically. Lastly, mechanical properties of two fixation methods for latarjet fixation surgery was evaluated. Endobuttons, which are known as agents that reduce the steps during surgery were compared with standard method of screw fixation.

In conclusion, two different medical equipment were 3D printed, and their mechanical properties were tested both with simulations and mechanical testing. Moreover, two ways to reduce aerosol load is proposed and evaluated during this thesis.

October 2021, 93 Pages

Key Words: 3D Printing, 3D Modelling, Covid 19, Laryngoscope, Mechanical Testing,

ÖZET

Yüksek Lisans Tezi

SARS-COV-II PANDEMİSİYLE MÜCADELEYE YÖNELİK 3 BOYUTLU BASKI TABANLI TEK KULLANIMLIK YARDIMCI TIBBİ ARAÇ-GEREÇ GELİŞTİRİLMESİ

Abdullah EYİDOĞAN

Ankara Üniversitesi
Fen Bilimleri Enstitüsü
Biyomedikal Mühendisliği Anabilim Dalı

Danışman: Prof. Dr. Pınar YILGÖR HURİ

SARS-CoV-II pandemisi ile mücadele amacıyla başlatılan bu tez çalışması, pandemi ile mücadelede bulaşma yollarından biri olan doktor-hasta ve hasta-hasta arasındaki bulaşma olasılığını azaltmayı amaçlamıştır. Bu kapsamda hekimlerin hastalarla temas halinde kullandıkları aletlerin ve hekimlerin kullandığı tüm bireysel koruyucu ekipmanların tek kullanımlık olarak hızla üretilmesi hedeflenmektedir.

Tez boyunca kişisel korunma ekipmanları (yüz siperleri) ve tedavi ekipmanları (laringoskoplar) 3B olarak yazdırıldı ve ticari olarak temin edilebilen muadilleri olarak performans gösterme kabiliyetleri test edildi. 3 tip yüz siperi değerlendirildi ve seçilen tip, üretilip binden fazla üretimle Covid19 ile mücadelede kullanıldı. Laringoskoplar için çeşitli tasarımlar, hem bilgisayarlı simülasyonlar hem de mekanik testler ile değerlendirilmiştir. Ayrıca, aerosol oluşumu azaltıcı iki yöntem mekanik özellikleri açısından test edilmiştir. Aort stent implantasyon cerrahisi için 3B basılı bir kılavuz oluşturmuş ve doğal dokuyu taklit etme yeteneği mekanik olarak test edilmiştir. Son olarak, laryenjet fiksasyon cerrahisi için iki fiksasyon yönteminin mekanik özellikleri değerlendirilmiştir. Cerrahi adım düşürücü ajanlar olarak bilinen endodügmeler, standart vida sabitleme yöntemi ile karşılaştırılmıştır.

Sonuç olarak, iki farklı tıbbi cihaz 3B olarak basılmış ve mekanik özellikleri hem simülasyon hem de mekanik testler ile test edilmiştir. Bu tez sırasında aerosol oluşumunu azaltmanın iki yolu önerilmiş ve değerlendirilmiştir.

Ekim 2021, 93 Sayfa

Anahtar Sözcükler: 3B Baskılama, 3B Modelleme, Covid 19, Laringoskop, Mekanik Test

ACKNOWLEDGEMENTS

First and foremost, I would like to express my sincere gratitude to my supervisor Prof. Dr. Pınar Yılgör Huri, to whom the words to describe her contribution to my personal development and my thesis could not be discovered by tens of thousands of years of human civilization.

I want to thank Prof. Dr. Çağdaş Oto, Orçun Güvener and MEDITAM for their precious supports during my thesis.

I am thankful to my colleagues Emre Ergene, Şeyda Gökyer, Ebru Talak, Meriç Göker and Mervesu Gökyürek for their support.

I would like to thank my precious friends M.Sc. Ceylan Demirci, M.Sc. Fırat Cem Savaş, B.Sc. Hatice Betül Bozdoğan, and B.Sc. Murat Şahin for their continuous help along my journey.

Finally, I am very grateful to my father Ferhat Eyidoğan, my mother Selma Eyidoğan, and my borthers Özgür Eyidoğans who are always around and willing to help me. The only way for me to be fortunate enough to complete my master's degree was with their support.

Abdullah EYİDOĞAN
Ankara, October 2021

INDEX

THESIS APPROVAL PAGE

ETHICS.....	i
ABSTRACT.....	ii
ÖZET.....	iii
ACKNOWLEDGEMENTS.....	iv
LIST OF ABBREVIATIONS	viii
LIST OF FIGURES	x
LIST OF TABLES	xiv
1. INTRODUCTION.....	1
2. LITERATURE SURVEY.....	4
2.1 3D Printing.....	4
2.1.1 History of 3D printers.....	4
2.1.2 Stereolithography.....	5
2.1.3 Fused Deposition Modelling.....	7
2.2 Preventive Efforts to Combat Covid-19 with 3D Printing	9
2.2.1 Face shields	9
2.2.2 Full protection masks.....	10
2.3 Diagnostic Efforts to Combat Covid-19 with 3D Printing	11
2.3.1 Nasopharyngeal swabs.....	11
2.3.2 Laryngoscopes	12
2.4 Therapeutic Efforts to Combat Covid-19 with 3D Printing	13
2.4.1 Ventilators.....	13
2.4.2 Ventilator parts	14
3. MATERIALS AND METHODS	16
3.1 Materials	16
3.1.1 Materials	16
3.1.2 Equipments	16
3.1.3 Softwares.....	16

3.2 Methods	17
3.2.1 3D model generation for face shields	17
3.2.2 3D model generation for laryngoscope	20
3.2.3 3D model creation from DICOM images	23
3.2.4 3D model generation of aorta parts	25
3.2.5 3D model slicing using CURA	28
3.2.6 3D model slicing using IDEAMAKER	30
3.2.7 Printing of models	32
3.2.8 Post processing applications	34
3.2.9 Compression strength characterization of 3D printed models	35
3.2.10 Tensile behavior characterization of 3D printed models	38
3.2.11 Three point bending characterization of 3D printed models	42
3.2.12 Mechanical evaluation of Screws and Endobuttons for Latarjet Fixation Procedures	44
4. RESULTS AND DISCUSSION	47
4.1 Face Shields	47
4.2 Laryngoscopes	52
4.2.1 Simulation of laryngoscope designs	52
4.2.2 Evaluation of laryngoscopes under compressive stress	63
4.2.3 Evaluation of laryngoscopes with three point bending test	63
4.3 Evaluation of Screws and Endobuttons	68
4.3.1 Evaluation of screws under tensile stress	69
4.3.2 Evaluation of Endobuttons under tensile stress	71
4.3.3 Comparison of screws and Endobuttons	74
4.4 Aorta Parts	77
4.4.1 Evaluation of aorta parts under compression stress	77
4.4.2 Evaluation of aorta parts under tensile stress	77
5. CONCLUSION	83
6. FUTURE PROSPECTS	85
6.1 Personal Breathing Unit	85

REFERENCES..... 86
CURRICULUM VITAE..... 91



LIST OF ABBREVIATIONS

.gcode	Geometric Code
.stl	Standard Triangle Language
1D	One Dimensional
2D	Two Dimensional
3D	Three Dimensional
ABS	Acrylonitrile Butadiene Styrene
cam/cad	Computer-Aided Design/Computer-Aided Manufacturing)
CNRS	French National Center for Scientific Research
COVID19	Corona Virus Disease 2019
CT	Computerized Tomography
DICOM	Digital Imaging and Communications in Medicine
ENT	Ear-Nose-Tounge
ENT specialists	Otolaryngologists
FDM	Fused Deposition Modelling
HIV	Human Immunodeficiency Virus
HU	Hounsfield Unit
k	Kilo
K wire	Kirschner Wire
kg	Kilogram
LASER	Light Amplification by Stimulated Emission of Radiation)
LED	Light Emitting Diode
M	Mega
MIMICS	Materialise Interactive Medical Image Control System
mm	Milimeter
MRI	Magnetic Resonance Imaging
N	Newton

Nylon	Now You Lazy Old Nippon
Pa	Pascal
PC	Poly Carbonate
PLA	Poly Lactic Acid
PPE	Personal Protective Equipment
PVC	Polyvinyl Chloride
SARS-CoV-II	Severe Acute Respiratory Syndrome Coronavirus 2
SLA	Stereolithography
SLS	Selective Laser Sintering
TPU	Thermoplastic Poly Urethane
UV	Ultra-Violet

LIST OF FIGURES

Figure 2.1 Scematic of Simple Stereolithography adapted from (webotonomfabrica 2021).	6
Figure 2.2 Diagram for Stereolithography CAD integration adapted from (weball3dp 2021).....	6
Figure 2.3 3D printing of human mandibula with SLA in our laboratory	7
Figure 2.4 Schematic representation of FDM.....	9
Figure 2.5 Computer-aided drawing of nasopharyngeal swab adapted from (Ford, Goldstein et al. 2020)	11
Figure 2. 6 Laryngoscope produced from metal and alloys.....	12
Figure 2.7 Picture of freely available laryngoscope design of airangelblade.org (dos Santos, de Melo et al. 2020).....	13
Figure 2.8 GlasVent System. a CAD model of GlasVent assembly, b System testing on a medical mannequin adapted from (Christou, Ntagios et al. 2020).....	14
Figure 2.9 a Dimensions, b final design, and c manufactured version of the two-port splitter adapted from (Ayyıldız, Dursun et al. 2020)	15
Figure 3.1 A picture of Faceshield produced for Ankara University Hospitals.....	17
Figure 3.2 Head covered main body design for face shields.	18
Figure 3.3 Reduced main body design for face shields.	18
Figure 3.4 Main body design for face shields	19
Figure 3.5 Multiple positioning of main body	19
Figure 3.6 Multiple positioning of reduced main bod.....	20
Figure 3.7 A picture of commercially available laryngoscopes for 3D design.....	21
Figure 3.8 Diagram for laryngoscope design.....	22
Figure 3.9 3D visualization of laryngoscope design.....	23
Figure 3.10 3D model creation of aorta from DICOM images.....	24
Figure 3.11 3D model of full aorta in the form of .stl.....	24
Figure 3.12 Selection of unnecessary parts.....	25
Figure 3.13 Removal of unnecessary parts	26
Figure 3.14 Final outcome to be printed	27
Figure 3.15 Representation of 3D printing in slices and assumingly 1D-->2D transformation	28
Figure 3.16 Slicing with 10 percent infill	29

Figure 3.17 Slicing with 20 percent infill	30
Figure 3.18 Shell number and shell crossing percentage	31
Figure 3.19 Extrusion width.....	31
Figure 3.20 Shell diameter calculation.....	32
Figure 3.21 3D printing with Ultimaker 2+	33
Figure 3.22 3D printing with Raise 3dpro	34
Figure 3.23 Post-processing of face shields	35
Figure 3.24 Universal testing device.....	36
Figure 3.25 Compression stress test.....	37
Figure 3.26 Compression test of laryngoscopes	37
Figure 3.27 Compression test of aorta parts.....	38
Figure 3.28 Tensile behavior test	39
Figure 3.29 Tensile behavior test of aorta parts	39
Figure 3.30 3D design of sample holder for tensile behavior test of aorta parts	40
Figure 3.31 Tensile behavior test of aorta parts with holder.....	41
Figure 3.32 Design of head of laryngoscopes for three point bending test.....	42
Figure 3.33 3D printing with 10% infill rate.....	43
Figure 3.34 3D printing with 25% infill rate.....	43
Figure 3.35 Three point bending test of 3D printed laryngoscope heads	44
Figure 3.36 Defect deciding.....	45
Figure 3.37 Fixation with endobuttons	45
Figure 3.38 Fixation with screws	46
Figure 3.39 Tensile tests using K wire.....	46
Figure 4.1 3D printed head covered face shield.....	47
Figure 4.2 3D printing procedure time of head covered main body	48
Figure 4.3 3D printed face shield.....	49
Figure 4.4 3D printed face shields in the help fight against Covid19.....	50
Figure 4.5 3D Printed face shields in the help fight against Covid19.....	51
Figure 4.6 3mm (mili meter) thickness and radius of 115mm sample under 100N force ...	53
Figure 4.7 3mm thickness and radius of 115mm sample under 200N force	53
Figure 4.8 3mm thickness and radius of 115mm sample under 400N force,	54

Figure 4.9 9mm thickness and radius of 115mm sample under 100N force	55
Figure 4.10 9mm thickness and radius of 115mm sample under 200N force.....	55
Figure 4.11 9mm thickness and radius of 115mm sample under 400N force.....	56
Figure 4.12 6mm thickness and radius of 115mm sample under 100N force.....	57
Figure 4.13 6mm thickness and radius of 115mm sample under 200N force.....	57
Figure 4.14 6mm thickness and radius of 115mm sample under 400N force.....	58
Figure 4.15 6mm thickness and radius of 100mm sample under 100N force.....	59
Figure 4.16 6mm thickness and radius of 100mm sample under 200N force.....	59
Figure 4.17 6mm thickness and radius of 100mm sample under 400N force.....	60
Figure 4.18 6mm thickness and radius of 130mm sample under 100N force.....	61
Figure 4.19 6mm thickness and radius of 130mm sample under 200N force.....	61
Figure 4.20 6mm thickness and radius of 130mm sample under 400N force.....	62
Figure 4.21 Summary of Simulations	62
Figure 4.22 Young modulus of laryngoscope head with different infill rates	64
Figure 4.23 Three Point Bending Test Results of 3D Printed Laryngoscope.....	64
Figure 4.24 Linear region of Three Point Bending Test Results of 3D Printed Laryngoscope.....	65
Figure 4.25 Samples before three point bending	66
Figure 4.26 Samples after three point bending	67
Figure 4.27 Samples during three-point bending.....	68
Figure 4.28 Tensile behavior characterization of Screw Sample1.....	69
Figure 4.29 Tensile behavior characterization of Screw Sample2.....	70
Figure 4.30 Tensile behavior characterization of Screw Sample3.....	70
Figure 4.31 Tensile behavior characterization of Screw Samples	71
Figure 4.32 Tensile behavior characterization of Endobutton Sample1	72
Figure 4.33 Tensile behavior characterization of Endobutton Sample2	72
Figure 4.34 Tensile behavior characterization of Endobutton Sample3	73
Figure 4.35 Tensile behavior characterization of Endobutton Samples	73
Figure 4.36 Tensile behavior characterization of Endobutton Samples and Screw Samples	74
Figure 4.37 Diagram for young modulus of Endobuttons and Screws.....	75
Figure 4. 38 Diagram for Ultimate Tensile Stress of Endobuttons and Screws	75

Figure 4.39 Diagram for Ultimate Tensile Stress of Endobuttons.....	76
Figure 4.40 Diagram for Ultimate Tensile Stress of Screws	76
Figure 4.41 Before the evaluation of aorta parts under tensile stress	78
Figure 4.42 During the evaluation of aorta parts under tensile stress	79
Figure 4.43 Tensile behavior characterization of Aorta Part Sample1	80
Figure 4.44 Tensile behavior characterization of Aorta Part Sample2	80
Figure 4.45 Tensile behavior characterization of Aorta Part Sample3	81
Figure 4.46 Tensile behavior characterization of Aorta Part Samples.....	81
Figure 4.47 Maximum elongation of Aorta Part Samples	82
Figure 4.48 Young modulus of Aorta Part Samples	82

LIST OF TABLES

Table 3.1 Materials.....	16
Table 3.2 Equipments.....	16
Table 3.3 Softwares.....	16



1. INTRODUCTION

This thesis study, which was initiated with the aim of combating the SARS-CoV-II (Severe Acute Respiratory Syndrome Coronavirus 2) pandemic, aimed to reduce the possibility of transmission between the doctor-patient and patient-patient, which is one of the ways of transmission in the fight against the pandemic. In this context, it is aimed to rapidly produce the tools used by physicians in contact with patients and all individual protection equipment used by physicians as disposable.

In this global pandemic that spreads through the air, such as COVID19 (Corona Virus Disease 2019), hospital tools and equipment are frequently used between patient-physician and patient-patient. Due to the fact that the material used on the patient could not be sterilized correctly and quickly, coronavirus was detected in a high number of healthcare workers, some of them died, and the inability to provide sterilization quickly caused significant disruptions in the treatment process of the patients.

The need for disposable sterile equipment will continue to be protected from the SARS-CoV-II virus, which is determined to be spread by the aerosol effect as well, and clinical units such as ENT (Ear-Nose-Tounge) specialists (otolaryngologists) and dentists working with cases that constantly produce aerosols will need the specified equipment for a long time (Gasmi, Noor et al. 2020).

SARS-CoV-II virus is stated the COVID19 pandemic and the virus had serious conflicting effects worldwide, the need for various sterile materials and protective equipment could not be met by exceeding the capacities of health institutions, and these products were priced high (Şahada, Tekindor et al. , Gereffi 2020). Since the impact of the epidemic could not be estimated so widely, there were significant problems in the design, manufacture, and supply of many cheap medical supplies in our country, high prices forced health institutions and bottlenecks occurred. This famine started with the inadequate supply of sterilized materials

used in healthcare institutions. Specific to the COVID19 epidemic, transmission occurs through the respiratory route (Somashkhar, Shivaram et al. 2020). Laryngoscopy is a procedure performed directly on the respiratory tract, and it is important for the control of the contamination chain that the material used to enter the respiratory tract, which is the focus of infection, is disposable. There is an urgent need for advanced imaging techniques such as CT (Computerized Tomography) and MRI (Magnetic Resonance Imaging) in cases of intensive care and interventional applications, respiratory tract infection, acute and complication situations in COVID19 patients (Edlow, Claassen et al. 2020). The laryngoscope is contraindicated for use in patients who require intubation during intubation or during advanced imaging. Therefore, disposable laryngoscopes designed from PLA (Poly Lactic Acid) can be used easily in CT and MRI (Lasprilla, Martinez et al. 2012).

With the COVID19 pandemic, too many people needed to intubate at the same time in hospitals (Yao, Wang et al. 2020). Since the endotracheal tube placed in the airway is changed several times with the intubation required for mechanical ventilation, laryngoscopy is performed more than once in the infected patient. The laryngoscope blade is metal and is a source of cross-contamination if not correctly cleaned and stored (Machan 2012). To stop the epidemic, it is necessary to break the transmission routes, destroy or adequately clean the infected device, and take personal precautions. In routine use, laryngoscopes that require mechanical cleaning and subsequent sterilization for reuse take 2-3 hours to be ready for use, and these preparations and waiting times cannot be achieved during an epidemic. It is important to produce disposable sterile laryngoscopes to address the increasing need for use and to eliminate the need for sterilization for reuse. With the disposable laryngoscopes for the needed use, the cleaning of the infected material by the health workers in the epidemic will be prevented, the contamination chain will be controlled by eliminating the possibility of laryngoscopes that cannot be cleaned properly as a source of crossover infection. Disposable laryngoscope etc. (Bowdle and Munoz-Price 2020). Equipment, especially for HIV (Human Immunodeficiency Virus), Hepatitis, Diphtheria, Pneumonia, etc. And after the COVID19 pandemic. It is important for the deterioration of the transmission route of diseases and emergency preparedness for physician health and public health.

The SARS-CoV-II global pandemic infected more than 20 million people at the time of this recommendation and caused the death of more than 750,000 people (Chavez, Long et al. 2021). The results of this thesis, which aims to develop protective equipment to combat this pandemic, will not only be specific to this pandemic, but will also benefit the rapid and effective creation of protection measures in possible pandemic processes.

This thesis proposed to be consist of a face shield, laryngoscope, individual breathing unit, and unseen possibilities to help the Covid19 pandemic. Along the thesis process, two more possibilities occurred to help the Covid19 pandemic. The first of these was to create 3D (Three Dimentional) printed guidance for aorta stents. This proposed 3D printed model for aorta parts are seemed to help the Covid19 pandemic. Since they will ease the work done by medical professionals and reduce the aerosol creation during the implantation of aorta stents. The other was the evaluation between surgical screws and endobuttons for latarjet fixation surgery. Hence endobutton, known as a reducer for surgery time it would seem like a helping agent for the fight against the Covid19 pandemic because it is obvious that less surgery time and step would mean less aerosol creation or less exposition against aerosols (Lu, Wang et al. 2016).

Unfortunately while including these two parts, we need to exclude the personal breathing unit due to financial inadequacy.

2. LITERATURE SURVEY

2.1 3D Printing

Fundamentally 3D printing is a way of creating an object with three dimensions. Sculptures create 3D objects from the beginning of time. 3D printing uses the approach of from bottom to top as the opposite of sculptures, which uses from top to bottom. With the from button to top, 3D printing basically takes 1D (One Dimensional) objects assumingly and creates assumingly 2D (Two Dimensional) objects, and it builds these 2D objects on top of each other and comes up with the desired 3D object.

2.1.1 History of 3D printers

Figuratively, the history of 3D printing begins with humans themselves. Maybe it can be even before humans if we considered bird nests etc., but the first tangible step towards the contemporary understanding of 3D printing can be accepted as the patent application of Dr. Hideo Kodama for rapid prototyping in 1980 (Lu, Wang et al. 2016, Su and Al'Aref 2018) . His proposed system was building of model layers via activation of photopolymer materials in a canister by UV light—this patent application and following two papers opened up the way to stereolithography.

In 1984 Jean-Claude André from the renowned CNRS (French National Center for Scientific Research) et al (Su and Al'Aref 2018). He Applied and received a local patent using the term of SLA (Stereolithography) three weeks before Chuck Hull, who actually shines up the SLA and is become well known for it. Jean-Claude André's this new invention was not considered valuable by CNRA, and their work did not continue.

In 1986, Chuck Hull, co-founder of nowadays one of the top 3D printing companies, granted a patent for SLA (André 2017). He used acrylic-based material, which was in liquid form at

the beginning of the process, which turns instantly solid with the application of UV (Ultra-Violet) light.

In 1988 Chuck Hull succeeded the commercialization of their product (Pastia 2021). This commercialization has fastened up the development of 3D printing.

In 1989 Carl Dekard, was an undergraduate student at that time, brought a patent for SLS (Selective Laser Sintering) (Wohlers and Gornet 2014)

Same year Scott and Lisa Crump got a patent for FDM (Fused Deposition Modelling) (Kamran and Saxena 2016, Grossin, Montón et al. 2021). The process basically uses melted thermoplastic material. This melted material becomes solid again with cooling down to create a 3D object layer by layer.

In 1992 Scott and Lisa Crump created the first operational FDM 3D printer and co-founded of nowadays one of the top 3D printing companies (Iuliano, Bondioli et al. 2019).

From 1992 to today and more on many 3D printers have been created and commercialized but all of these mainly used previously mentioned two technologies which are Stereolithography and Fused Deposition Modelling.

2.1.2 Stereolithography

Stereolithography is a way of 3D printing. It goes from 2D to 3D by using layer by layer technology which means slicing of a 3D object, and instead of creating a 3D object at once, the creation of 3D objects first layer and the second layer on top of it and more on. In stereolithography base, the material for the object should be photosensitive (Hull 2012). A light source is used to turn photosensitive material from the liquid into a solid form. Adding of the each layer on each other creates the whole 3D model.

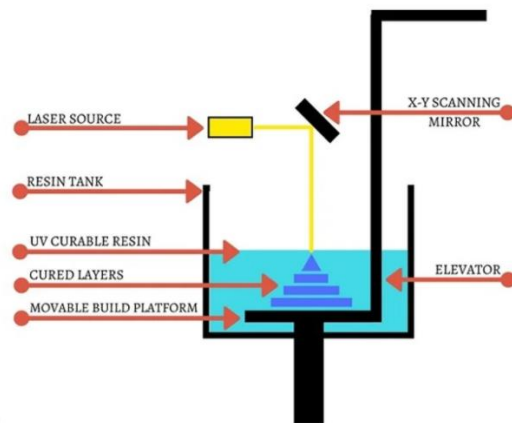


Figure 2.1 Schematic of Simple Stereolithography adapted from (webotonomfabrica 2021).

Basic schematic of a contemporary stereolithography system (Figure 2.1). The material should be photosensitive. Laser source creates the lights to turn photo sensitive material from solid to liquid. Elevator helps the system go above and create the upper layers.

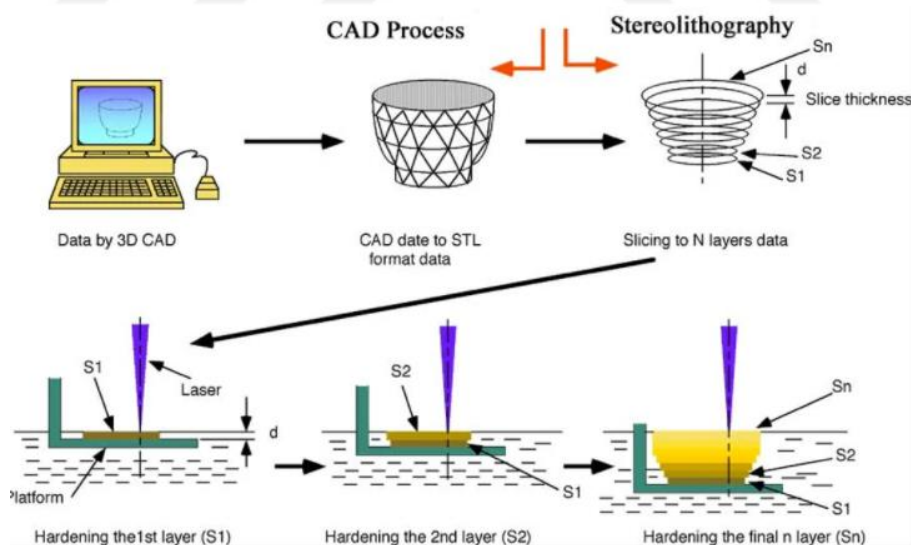


Figure 2.2 Diagram for Stereolithography CAD integration adapted from (weball3dp 2021)

Nowadays, SLA is integrated with computer-aided design systems, which helps the precision and increases the efficiency of the process. The main workflow of a computer-aided SLA system is given in (Figure 2.2).

First of all, in this system 3D, solid data acquired from computers could be either designed from ideas or captured from real life and turned into a virtual environment. The most common file format for 3D solid data is .stl (Standard Triangle Language), which comes from stereolithography and is named standard triangle language. 3D solid data sliced by computer into assumingly 2D parts. Each of these parts (layers) starting from the bottom later printing out by hardening photosensitive material with laser application. In each LASER (Light Amplification by Stimulated Emission of Radiation) affects only the necessary regions; hence the rest stays in liquid form. After the printing of all layers, excess resin is removed from the solidified 3D object. Lastly desired 3D object is formed. A picture of the final product of SLA printing from our lab is given in (Figure 2.3).



Figure 2.3 3D printing of human mandibula with SLA in our laboratory

2.1.3 Fused Deposition Modelling

Fused Deposition Modelling is a method that melts the filament material pushed from behind with the help of the heater, and this molten material is cast to the desired places on the

platform with the use of nozzles and motors and the software at the back, and it is a method for establishing complex structures (Yeong and Chua 2014, Gökyürek 2020). The most commonly used materials are polymer group materials such as PLA, ABS (Acrylonitrile Butadiene Styrene), TPU (Thermoplastic Poly Urethane), but with this method, it can be applied to a variety of materials such as metals. Basically, and in the most used form, while the motor and nozzle move in the XY plane, the platform at the end of the layer moves as much as the layer thickness in the -Z-direction, and the construction of the second layer continues. Since the structures are built layer by layer, these layers can form a strong bond with each other only when they reach the appropriate temperature. For this reason, the most effective parameter of this process is temperature, and temperature control is vital in the process. If it is not melted enough and solidification occurs without establishing a bond, the interlayers will not be strong. If there is a scorching environment, this time, the solidification process will be slow, and there may be a defect in the structure. A schematic of FDM is given below (Figure 2.4).

The purpose of using FDM technology is usually the production of a prototype or mechanical test measurements. The mechanical test measurements here are generally lower than the materials produced by injection, but they give an idea about the material and structure. If it is considered as a material since the outer surfaces cool quickly and the inner side of the print will cool more slowly when printing with injection, the grain sizes of the outer surface will be small, and the grain sizes of the inner parts will be larger. However, when printing with FDM, there is no grain size difference between the inside and outside of the print since all places are cooled equally so that the desired grain size can be reached in the material (Singh and Ranjan 2018). The internal and external characteristics of the material are equalized.

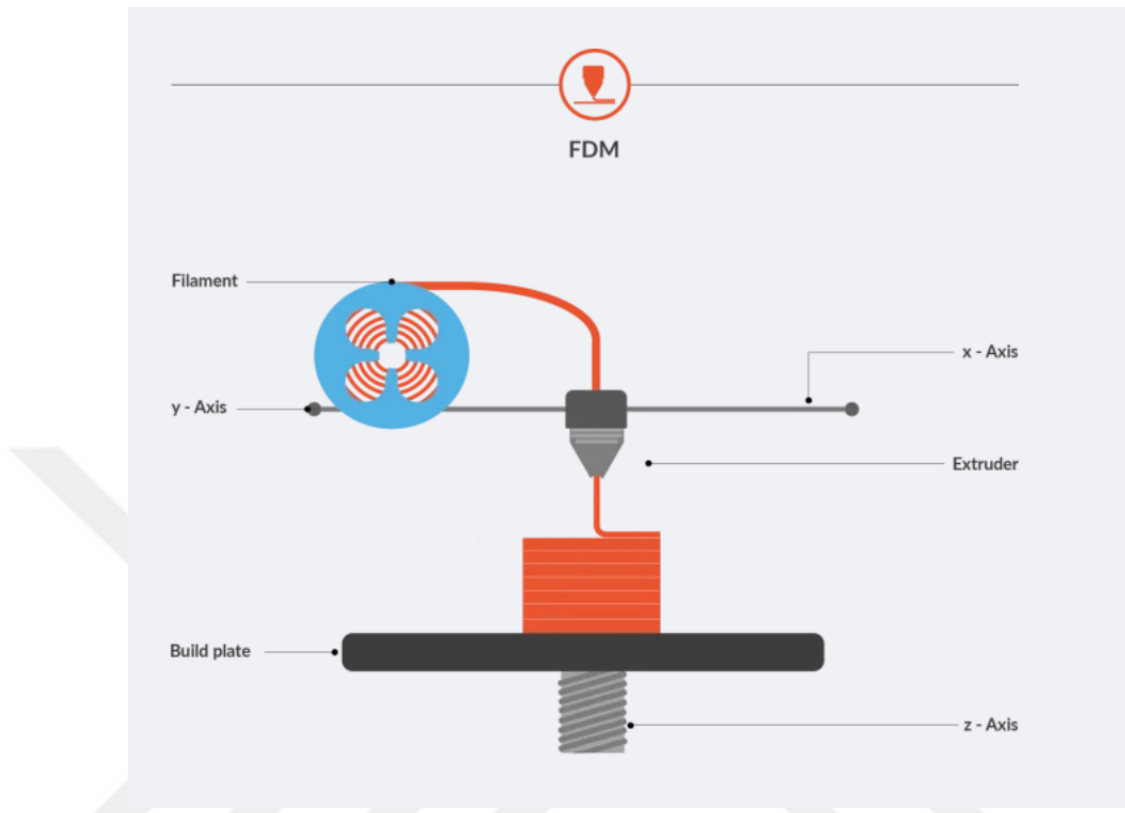


Figure 2.4 Schematic representation of FDM

2.2 Preventive Efforts to Combat Covid-19 with 3D Printing

During the Covid-19 epidemic period, masks and shields are 3D printed and become at the top of the list of increasing PPE (Personal Protective Equipment) demands (Rendeki, Nagy et al. 2020). For this reason, here, the approaches required for the production of apparatus are presented in their most general form by dividing them into two main design types, brief information is given about the production methods, and at the same time, the efficiency of use is explained.

2.2.1 Face shields

Shields alone does not provide complete protection but are suitable barriers. They reduce the risk of contamination in environments where aerosol generation is intense . A face shield;

the frame consists of three simple parts. The first part is an elastic band. This band helps to fasten the shield around the head. The last part is a clear plastic visor which both prevents infection and creates a clear image. It is advantageous in terms of parameters such as fast production, ease of disinfection, and comfort of use. Although the choice of the plastic visor is not very special, any transparent plastic sheet can be used as a visor. The use of PVC (Polyvinyl Chloride) film as an option for visor because it is soft for shaping and has enough ductility to preserve the needed shape. The face shields are reusable by replacing the visor. Moreover, the visor can be used for more than one day if appropriately sterilized (Amato, Caggiano et al. 2020).

2.2.2 Full protection masks

First of all, computer-aided software is used to obtain the virtual model, and after various desired changes are made, the model is saved in the .stl form, which is specific for 3D modeling. The saved .stl is needed to slice with a slicer program. From here, it is converted into a .gcode (Geometric Code) file form. A 3D printer can use the .gcode file form to print out 3D models. As explained earlier, there are many ways for 3D printing. For PPE production, producing style needs to be medically safe. PPE production is carried out with plastic powders using SLA or SLS techniques. These plastic powders are either resin or petroleum-based materials. In order to eliminate the dangers that may arise during use due to the materials used during production, it may be necessary to use protective medical coating layers on the products produced to prevent contact with the skin (Liao, Liu et al. 2021). Since it works with a PLA filament. PLA filament is known as biocompatible. The FDM approach is emerging as an alternative approach to address the concern mentioned above. Nylon (Now You Lazy Old Nippon) filaments are often preferred for the production of more elastic parts. Various studies also show that the method used is a low-cost method. It is also reliable and fast.

2.3 Diagnostic Efforts to Combat Covid-19 with 3D Printing

2.3.1 Nasopharyngeal swabs

There are two common ways to diagnose Covid19. The first one is the medical imaging of possibly infected tissues. The second one is specimen gathering from the pharyngeal tissues. For this operation, a piece of helping medical equipment was used, named a nasopharyngeal swab. This swap seems easy to produce with 3D printing a 3D design of these swaps is given in (Figure 2.5).

Using 3D printers in the medical industry requires several must-to-do. First of all, the material to be used has to be biocompatible. PLA is one of the most known biocompatible materials to be used in 3D printing. Another important issue is either sterilize the producing area or being able to sterilize the materials after 3D printing. PLA is compatible with the most common way of sterilization that is used in the medical industry, which is ethylene dioxide sterilization (Meglioli, Toffoli et al. 2020). This obvious ability of 3D printers set in motion many of the world's leading companies in the 3D printing and medical industry. With the organization of those companies and the help of communities of 3D printing, millions of these swaps are 3D printed and used in the fight against Covid19.

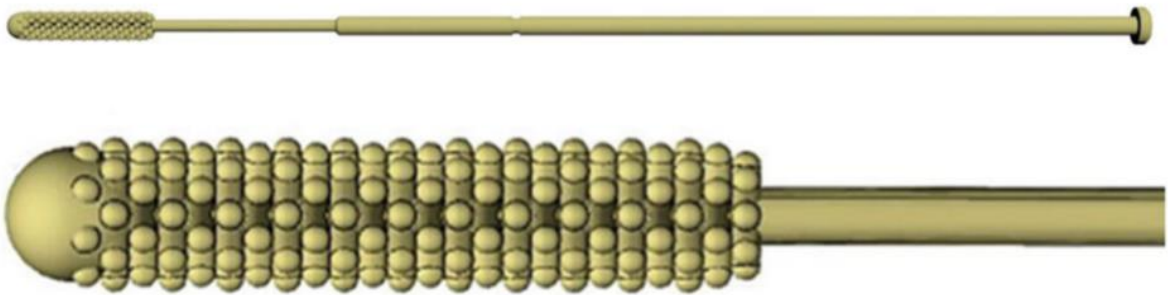


Figure 2.5 Computer-aided drawing of nasopharyngeal swab adapted from (Ford, Goldstein et al. 2020)

2.3.2 Laryngoscopes

Laryngoscopes are used for the intubating of mammals when their lungs are unable to perform with satisfaction. Normally laryngoscopes are industrially produced using metal alloys (Figure 2.6).

Normally these devices are used for one person during the day and they are sterilized before the next patient. This sterilization process takes 8 hours to one day in relation to hospitals' capacity and ongoing sterilization procedures (Juwarkar 2013).



Figure 2.6 Laryngoscope produced from metal and alloys

Since it is very important to use one device for more than one patient during pandemics, hospitals were needed the bought many of these industrial laryngoscopes. Due to the scarcity of laryngoscopes in the market, 3d printing of these devices has become popular (Chepelev and Rybicki 2021). One popular design is created by airangelblade.org given in the figure 2.7 and given free usage for a fast and effective fight against the pandemic (AO 2021).



Figure 2.7 Picture of freely available laryngoscope design of airangelblade.org (dos Santos, de Melo et al. 2020)

2.4 Therapeutic Efforts to Combat Covid-19 with 3D Printing

Since the start of the Covid19 pandemic, 3D printing has been a helping agent in the fight against the pandemic. It is used for the production of therapeutic devices. Moreover, existing devices are either upgraded or reproduced utilizing this technology (O'Dowd, Nair et al. 2020). Various types of aides have been produced by 3D printing. These include disposables and practical frameworks

2.4.1 Ventilators

It is known that SARS-CoV-II infection is more active in the lungs (Boutin, Hildebrand et al. 2021). This is due to the humidity of the tissue of the lungs. Hence the respiratory system is affected by the virus in most patients. As just like other infections, the virus penetrates a healthy cell and uses this cell to produce new virus parts. After that, the virus moves through the mucous environment and comes to the lungs, where the virus has the most dangerous impact. When lungs are not working accordingly, oxygen saturation starts to decrease. If oxygen saturation drops below 95%, physicians recommend artificial help for respiration (Mlcak, Suman et al. 2007). Furthermore, when oxygen saturation goes below 90%, artificial

support is mandatory. Mechanical ventilators provide artificial assistance for respiration. These mechanical ventilators control crucial parameters such as tidal volume, airway pressure, and respiration rate. However, during the COVID-19 pandemic, ventilator need was increased, and available stocks were not enough to supply this need (Ranney, Griffeth et al. 2020). Because of these reasons, most companies worldwide are focused on the fast production of these medical devices. Besides, researchers focused on low-cost, uncomplicated, and easy types of artificial respiration devices (Figure 2.8).

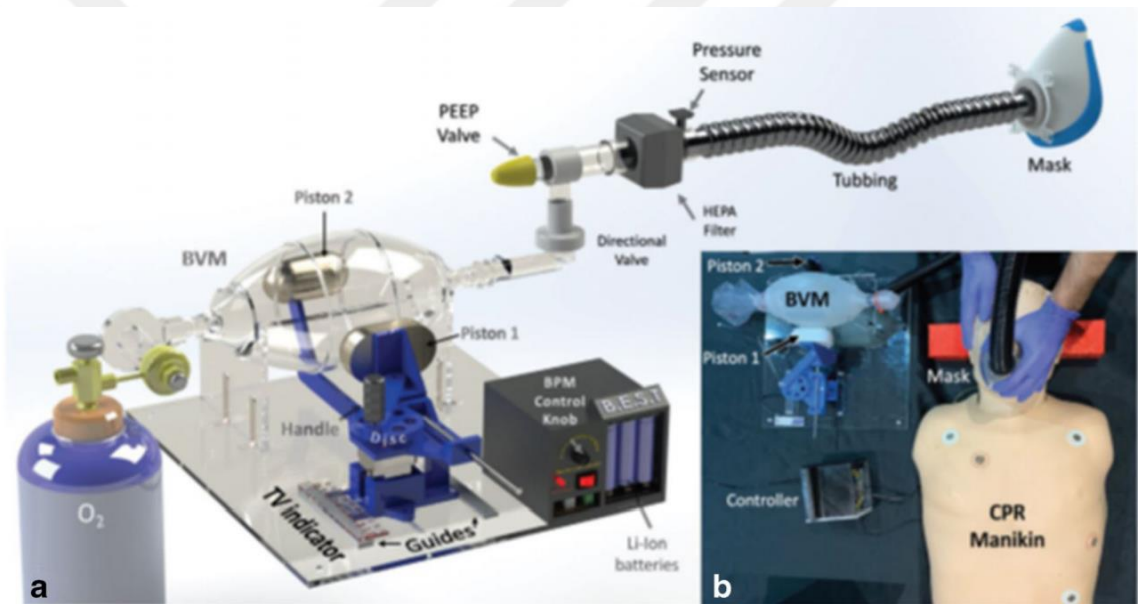


Figure 2.8 GlasVent System. a CAD model of GlasVent assembly, b System testing on a medical mannequin adapted from (Christou, Ntagios et al. 2020)

2.4.2 Ventilator parts

Because of a scarcity of mechanical ventilators, the ventilators are intended to be used by more than one person. And this idea is tested by Greg Neyman and Charlene Babcock Irvin (Guvener, Eyidogan et al. 2021). Due to the split of airways, T-tubes were used. Although four lung simulators are used successfully in this test, it does not provide sufficient information about oxygenation. In another study, four sheep, around 70 kg are ventilated

using mechanical ventilators and commercial manifolds. In this study, even though four sheep successfully ventilated for 12 hours, there was no study about differential lung compliance or cross-contamination.

For COVID-19, in light of these studies, these manifolds were designed with polyjet technology for humans (Figure 2.9). Two intensive care specialists with the same weights use the same mechanical ventilator that is designed for humans at the same time. During this study, the mechanical ventilator gave errors frequently in synchronized mode and almost continuously in non-sync mode (Ayyıldız, Dursun et al. 2020, Guvener, Eyidogan et al. 2021). For this reason, this study showed that the usage of one mechanical ventilator needs to be synchronized. Under the difficult circumstances, two patients can share one mechanical ventilator for short period, but this is inappropriate.

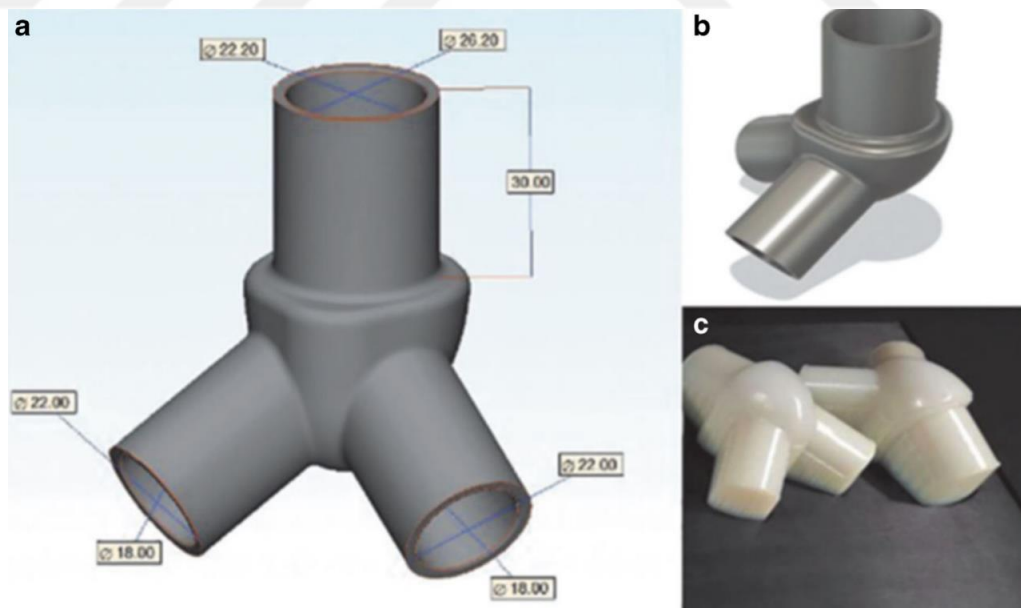


Figure 2.9 a Dimensions, b final design, and c manufactured version of the two-port splitter adapted from (Ayyıldız, Dursun et al. 2020)

3. MATERIALS AND METHODS

3.1 Materials

3.1.1 Materials

Table 3.1 Materials

Material	Brand Name	Usage
PLA Filament	Esun and Raise Premium	3D Printing
Acetate Paper	Komex	Face Shield
TPU Filament	Raise	3D Printing of Aorta

3.1.2 Equipments

Table 3.2 Equipments

Equipment	Brand Name	Usage
Universal Mechanical Tester	Schimidzu	Mechanical Tests
Ultimaker 2+	Ultimaker	3D printing
Raise 3dpro	Raise	3D Printing

3.1.3 Softwares

Table 3.3 Softwares

Software	Brand Name	Usage
Autocad	Autodesk	3D design
Mimics	Materialise	DICOM
Cura	Ultimaker	.gcode creation
Inventor	Autodesk	3D design and virtual analysis
Ideamaker	Raise	.gcode creation
Meshmixer	Autodesk	3D design

3.2 Methods

3.2.1 3D model generation for face shields

3D model generation for face shields has been done using Autodesk®'s Autocad cam/cad (Computer-Aided Design/Computer-Aided Manufacturing) program. Face shields designed for emergent response to Covid19 pandemic consisted of 3 main parts main body, main body head attachment, and protective shield as given in (Figure 3.1). These parts can be identified by color codes being main body as a white, main body-head attachment as turquoise, and protective shield as transparent.



Figure 3.1 A picture of Faceshield produced for Ankara University Hospitals

Out of these three parts, only the main body is 3D printed. The others were gathered from open market suppliers. Actually, the main body consists of two parts which are the main body and clamps. During the main body design process three different model were designed which are main body (Figure 3.4), reduced main body (Figure 3.3), and head covered main body (Figure 3.2).

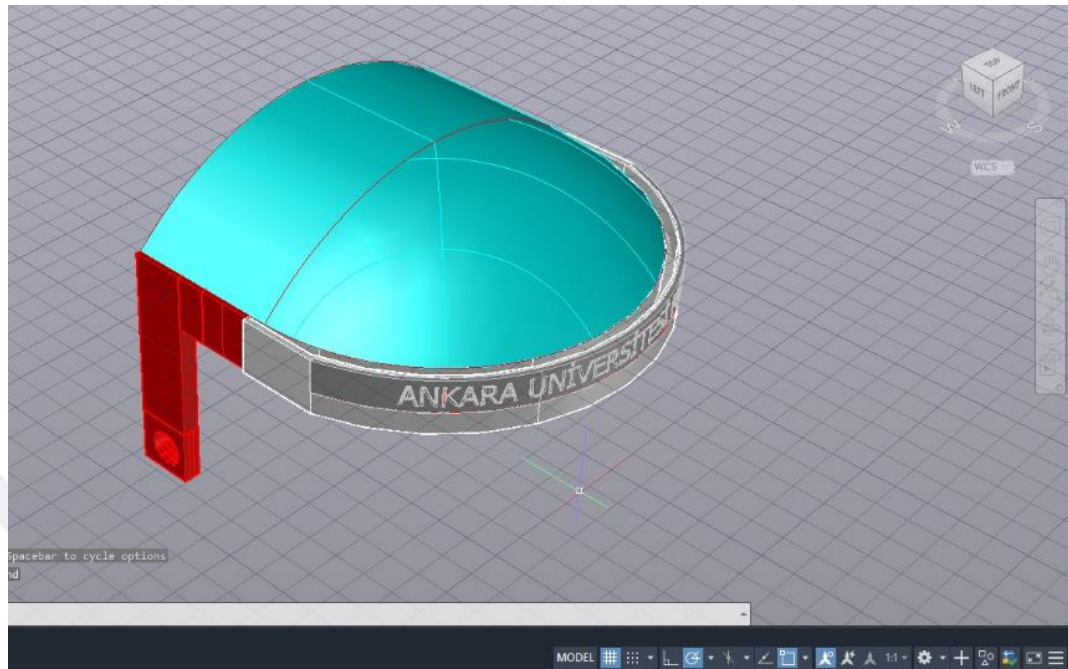


Figure 3.2 Head covered main body design for face shields

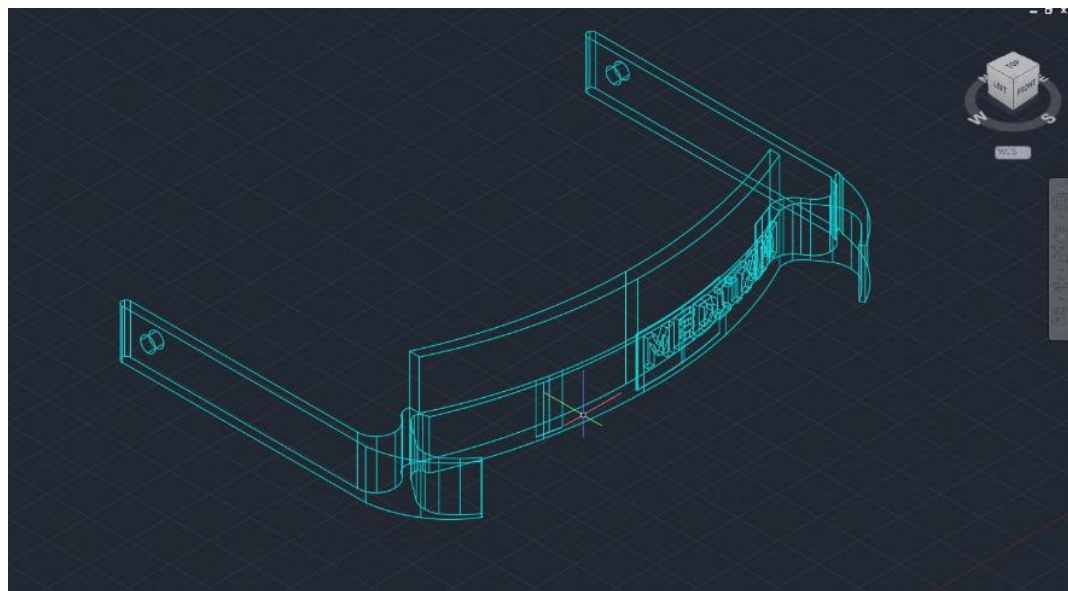


Figure 3.3 Reduced main body design for face shields

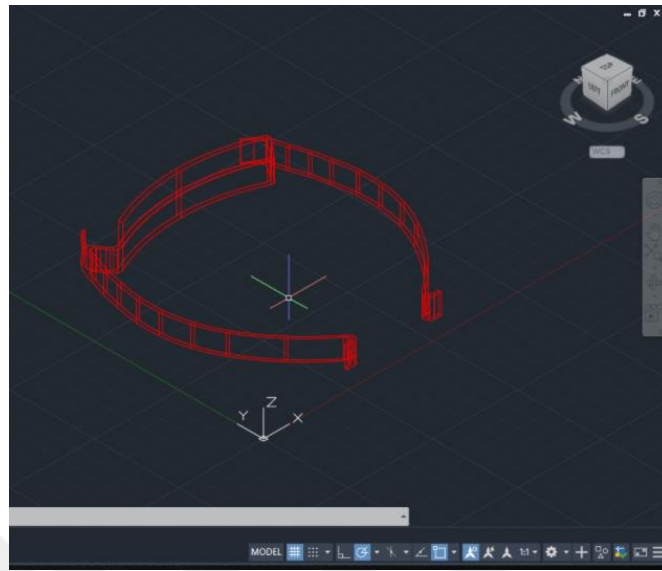


Figure 3.4 Main body design for face shields

Rather than main body designs, two different multiple 3D body positionings have been designed for better printing performance. The first design is consists of 3 reduced main bodies (Figure 3.6), and second design is consists of 13 main body (Figure 3.5).



Figure 3.5 Multiple positioning of main body

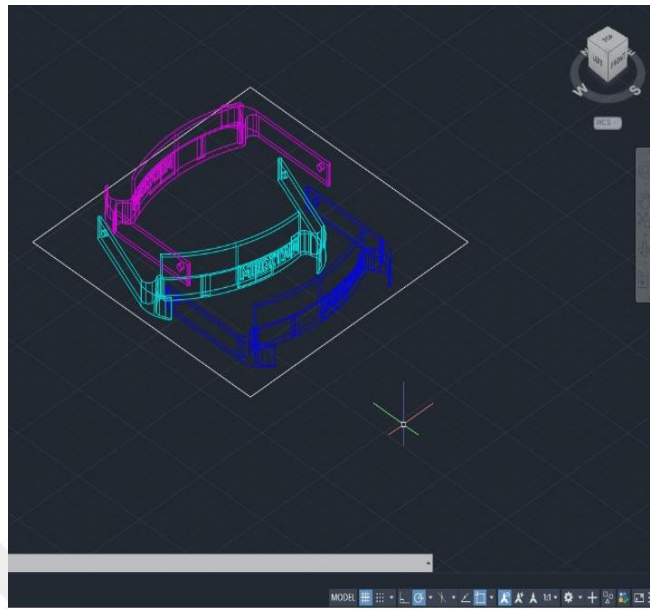


Figure 3.6 Multiple positioning of reduced main bod

3.2.2 3D model generation for laryngoscope

3D model generation for laryngoscopes has been done using Autodesk®'s Autocad cam/cad program. The design process is inspired by the commercially available metal-based laryngoscope. The laryngoscopes picture (Figure 3.7) is gathered from the Thoracic Surgery Department of Ankara University.



Figure 3.7 A picture of commercially available laryngoscopes for 3D design

Laryngoscopes designed for emergent response to Covid19 pandemic was consist of two main parts, which are laryngoscope's body and electronic parts for light. Laryngoscopes body is consists of 7 different design elements. All of these parts are designed to print all together as a part of the whole body. These parts are symbolized with color codes (Figure 3.8). The turquoise part has a cylindrical shape and is used as a first touching point for medical professionals to the patient tongue. Its dimensions have been changed after the reviews from the medical professionals of the Thoracic Surgery Department of Ankara University. The blue part is the main angled part of the laryngoscope, and it covers all of the human's tongue during intubating process its angle has been redesigned after the reviews from the medical professionals of the Thoracic Surgery Department of Ankara University. Since it is the main load-bearing part of the device, it has been supported with the yellow labeled parts for better performance. The yellow part is an angled hollow for the LED (Light Emitting Diode) lamps cables between lamb and battery. The LED lamps are chosen for the laryngoscope due to

their fewer heat emissions. The red area is designed for the support of an LED lamp. A gray area is for holding part of the laryngoscope, and it is designed in both rectangular prism (for quick and efficient printing) (Figure 3.9) and cylindrical form (for better holding ergonomics) (Figure 3.8). The black part is designed for battery housing, and purple part is designed for the activation button.

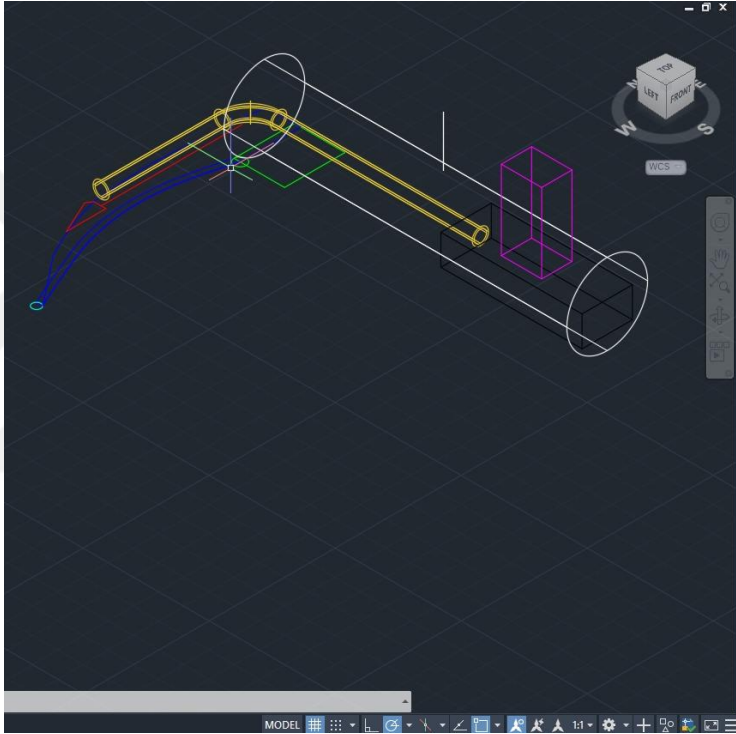


Figure 3.8 Diagram for laryngoscope design

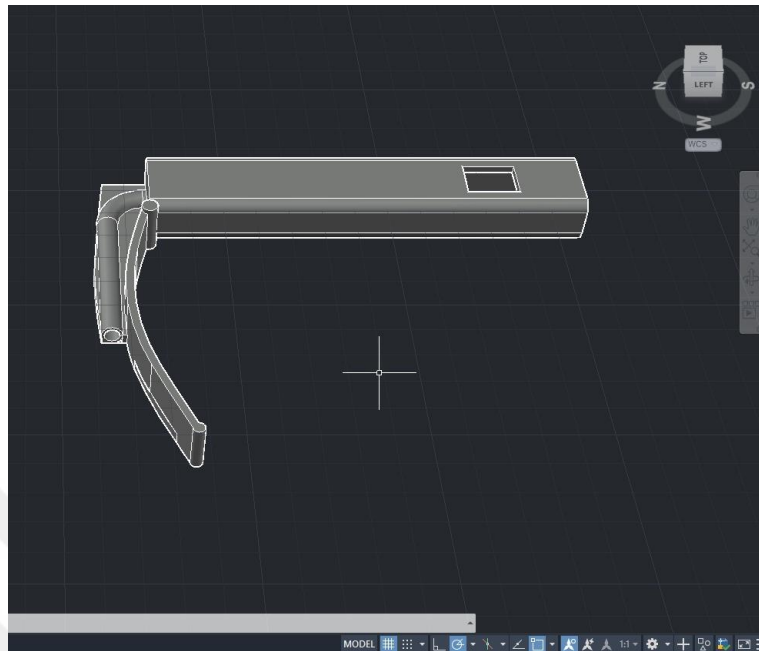


Figure 3.9 3D visualization of laryngoscope design

3.2.3 3D model creation from DICOM images

3D model creation from DICOM (Digital Imaging and Communications in Medicine) images has been done using Materialize®'s MIMIC's (Materialise Interactive Medical Image Control System) cam/cad program. To be able to gather aorta 3D model, an open accessed computerized tomography data is used. A CT data includes information about all body parts as bones, veins, neurons, organs, and other tissues. A specific separation is needed to remove aorta data from the other tissues. For this separation, there is a tool named after Sir Godfrey Hounsfield, which is HU (Hounsfield Unit). HU is a dimensionless number. HU is calculated with a linear configuration of the attenuation coefficient of each tissue (T_u , Inthavong et al. 2012). Since each tissue has a different water concentration, its attenuation coefficient becomes dimensionless with HU for universal usage. In the given figure (Figure 3.10) we can see an applied threshold of HU from 226 to 3071, which is commonly used for bone-in adult males. By applying the correct thresholds and using the coronary aid tools in the MIMICS program aorta is separated from the whole CT with its helping veins and arteries as in (Figure 3.11).

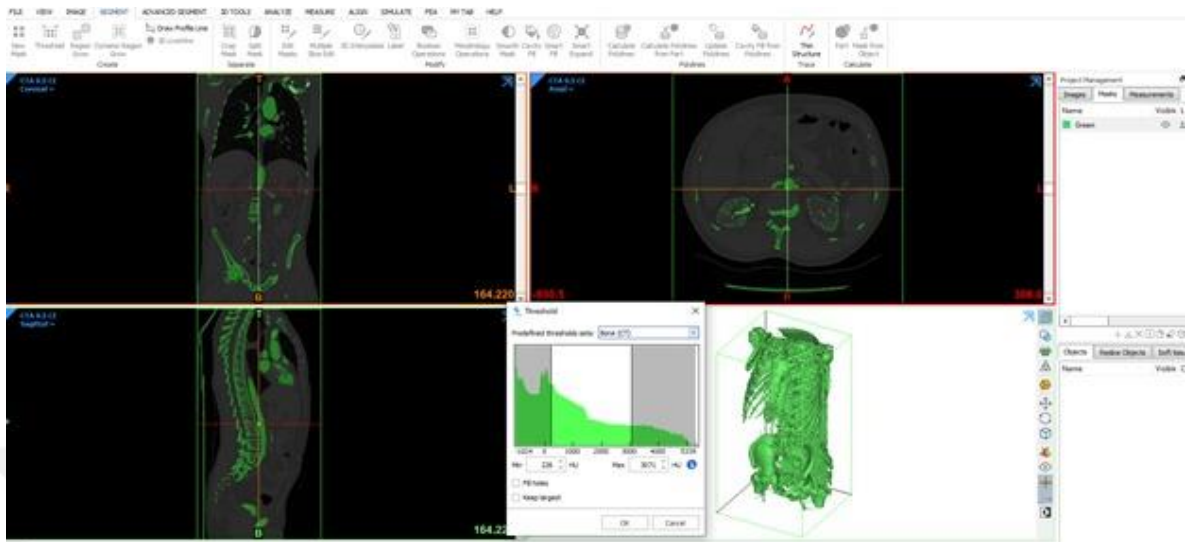


Figure 3.10 3D model creation of aorta from DICOM images

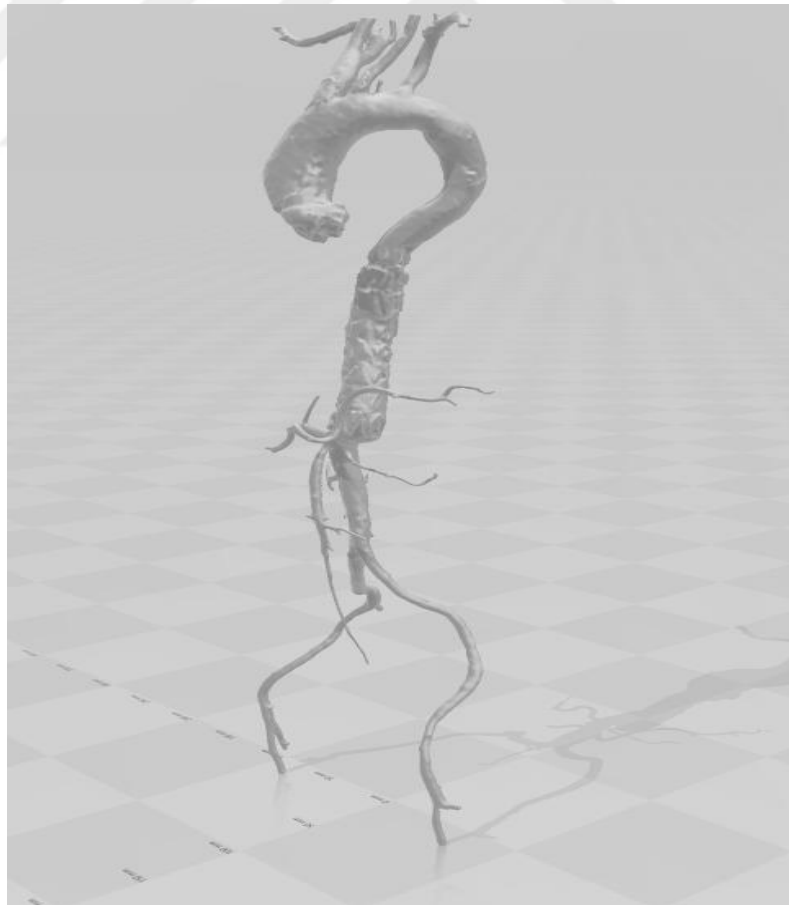


Figure 3.11 3D model of full aorta in the form of .stl

3.2.4 3D model generation of aorta parts

3D model generation for aorta parts has been completed using Autodesk®'s Meshmixer cad/cam program. 3D printing of all aorta as in the given figure (Figure 3.11)) means both time and expendables unnecessary usage. Hence unnecessary parts of the aorta are decided with medical professionals and removed from the 3D model. The removing process is straightforward. It only includes selecting unnecessary parts as in (Figure 3.12) and deleting those parts from selection lists as in (Figure 3.13). Finally, the outcome would be ready for 3D printing as in (Figure 3.14).

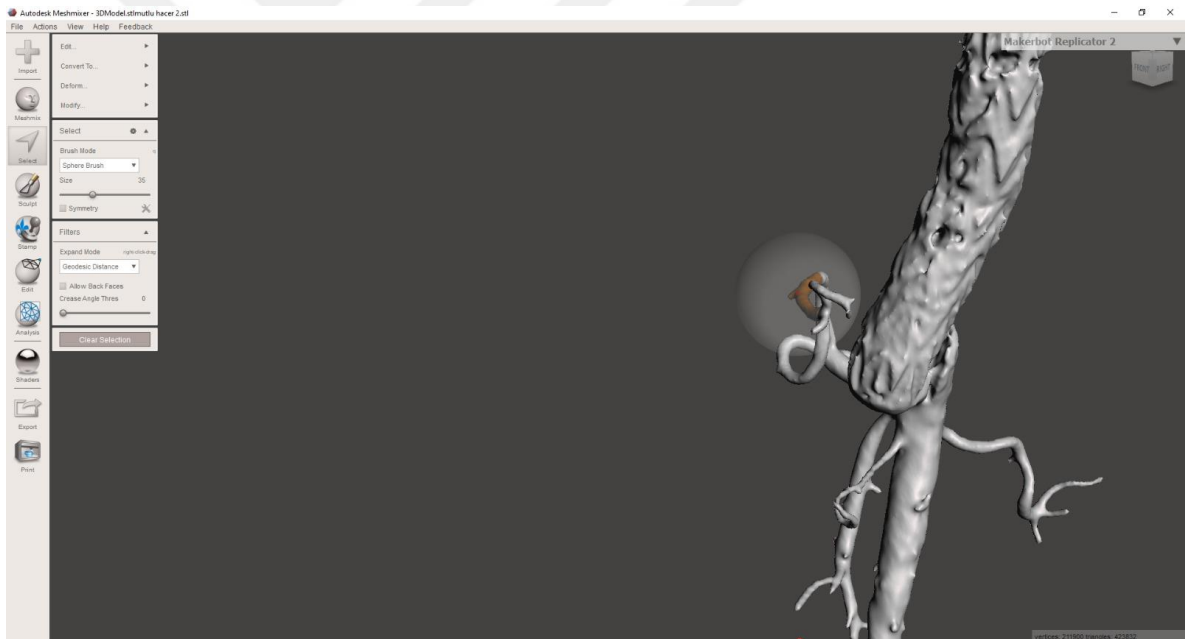


Figure 3.12 Selection of unnecessary parts



Figure 3.13 Removal of unnecessary parts

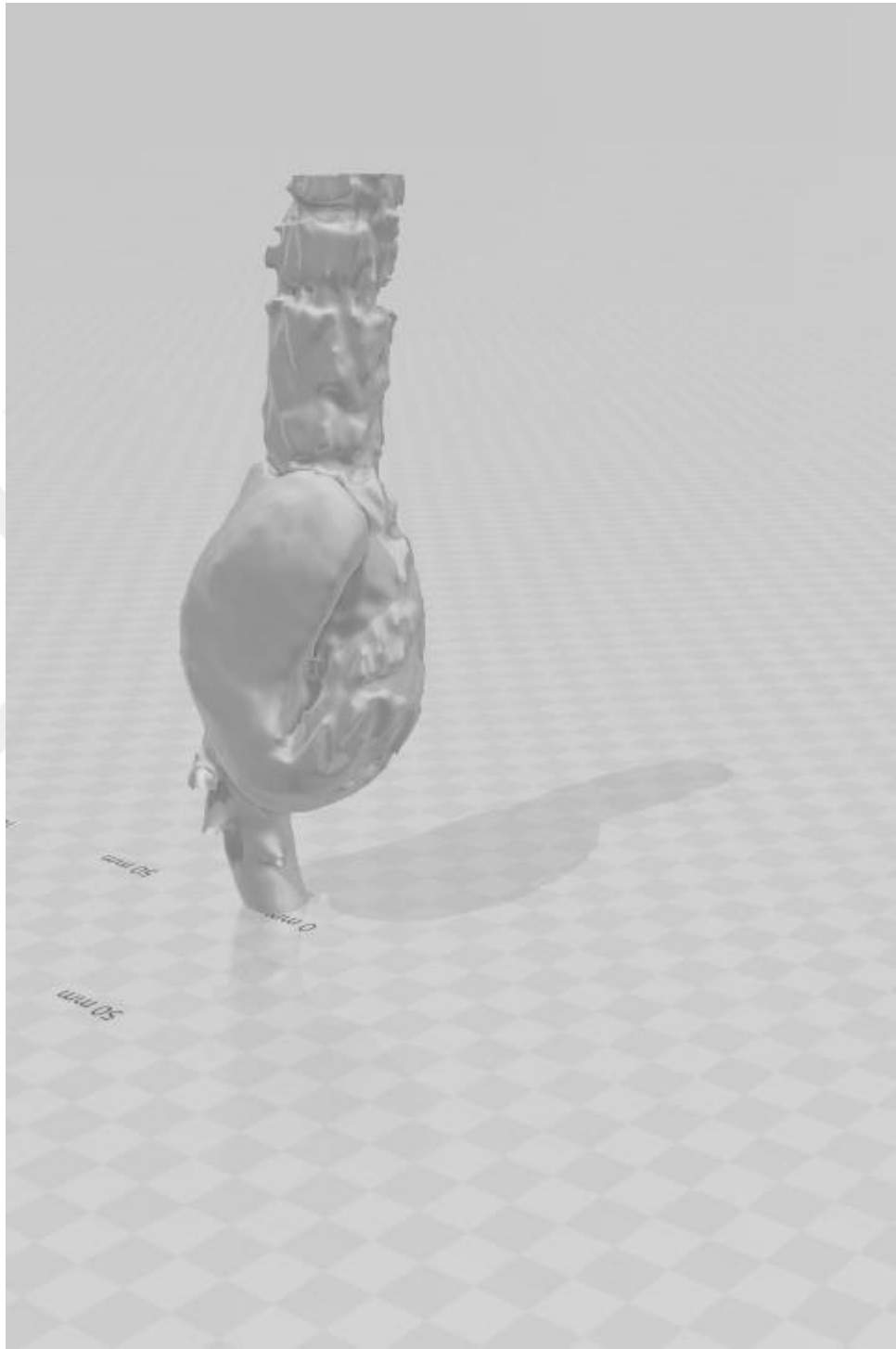


Figure 3.14 Final outcome to be printed

3.2.5 3D model slicing using CURA

Designed 3D models needed to be sliced into assumingly 2D formation and printed out on top of each other. There are several slicing programs slicing of both face shield main bodies and laryngoscopes have been done using the CURA® program. This program does not only slices the 3D model into 2D parts but also creates patterns for the nozzle to move in x/y directions as in (Figure 3.15). This can be thought of as 2D from 1D.

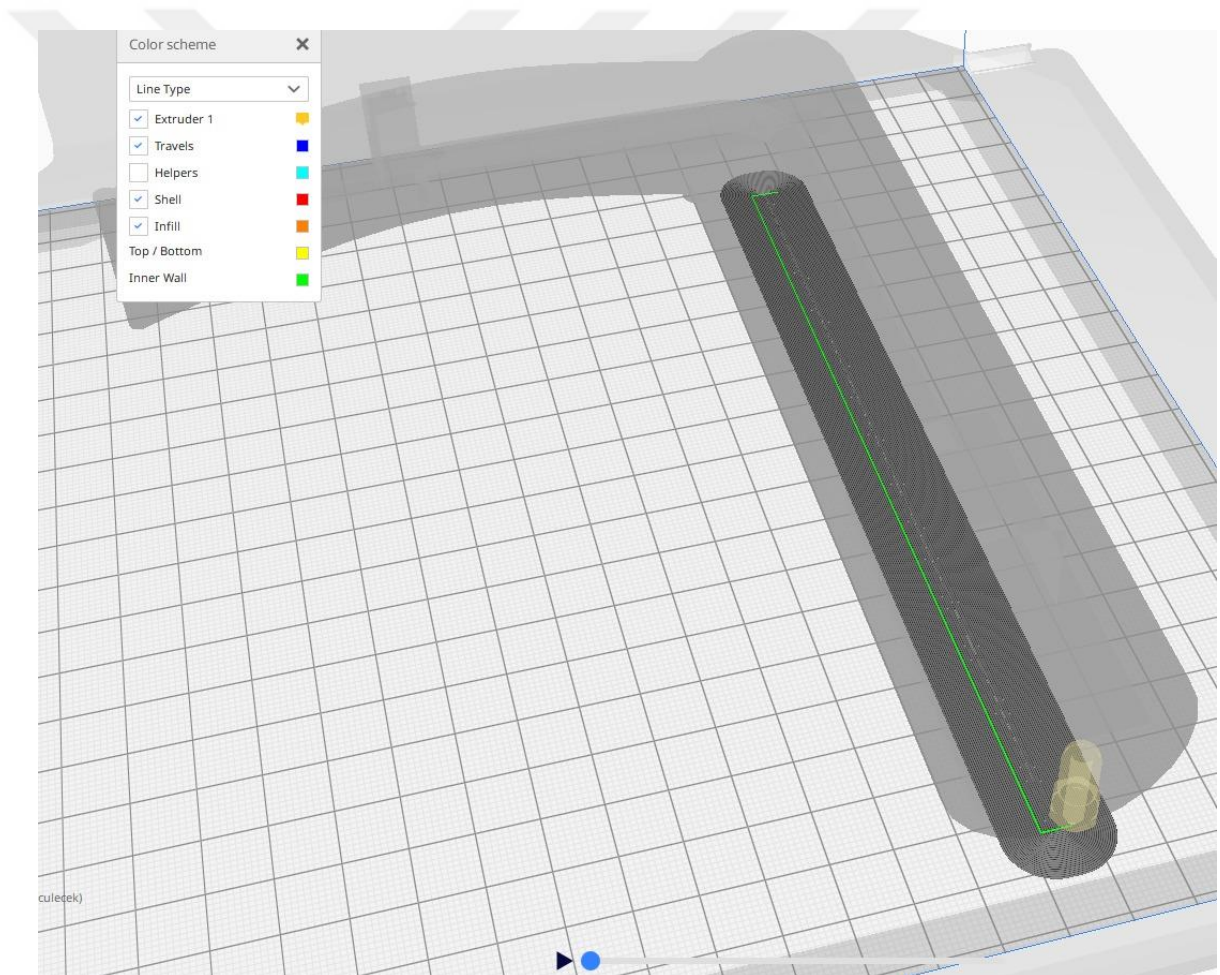


Figure 3.15 Representation of 3D printing in slices and assumingly 1D-->2D transformation

The Cura® program combines this x/y movement data of each slice with each other a file with a .gcode ending which is the primary file type for the operation of contemporary 3D printers. The .gcode file includes slicing, movement, material type, nozzle diameter, infill rate of the model, movement speed, several helpers and support, the diameter of the shell of the 3D model, heating temperature for the nozzle and building plate, and countless of other features depends on the printer model. In this study, 3D models are sliced for Ultimaker 2+ 3D printer using PLA and PC (Poly Carbonate) polymers and using default printing features for normal quality. The only change in the printing parameters is the change of infill rate (Figure 3.16-18) to optimize the printing time and mechanical properties needed for the usage. Infill rates of 10 %, 20 %, 40 % are used for 3D printing of both PLA and PC samples of laryngoscopes.

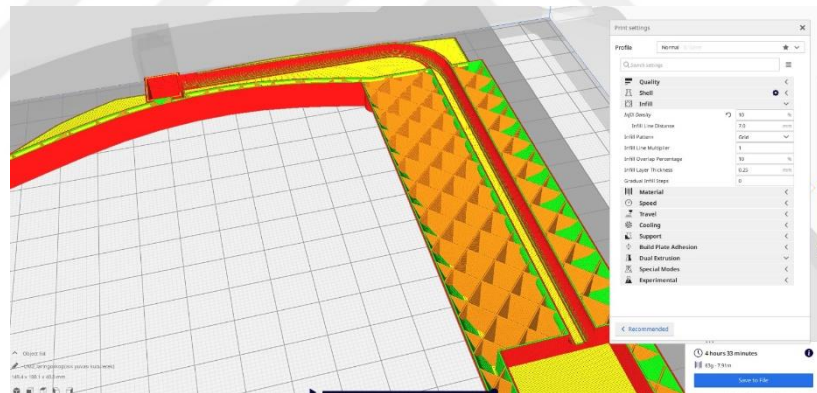


Figure 3.16 Slicing with 10 percent infill

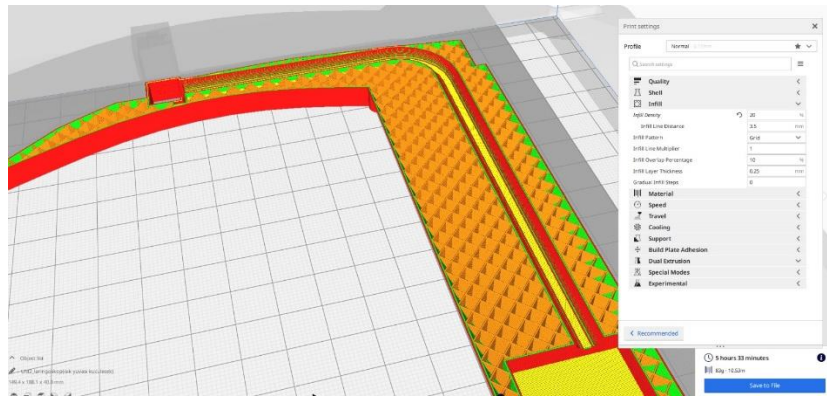


Figure 3. 17 Slicing with 20 percent infill

3.2.6 3D model slicing using IDEAMAKER

There are several slicing programs, slicing of aorta model have been done using IDEAMAKER® program. The change in the slicing program was due to the difference in the printers. Many slicing programs can be used to slice for other types of 3D printers rather than their own manufacturers. Hence, Cura can slice for Raise 3dpro type of 3D printers, but Ideamaker, which is designed for Raise 3dpro, performs better than Cura. Thus, both Ideamaker and Raise 3dpro are from the same manufacturers. The slicing parameters used in the Ideamaker same as Cura, which is the default normal printing quality with differences in infill rate with 10 %, 20 %, and 40 % changes. The only difference was the fixation of shell diameter to 1mm to mimic the human body more effectively (Figure 3.18-20).

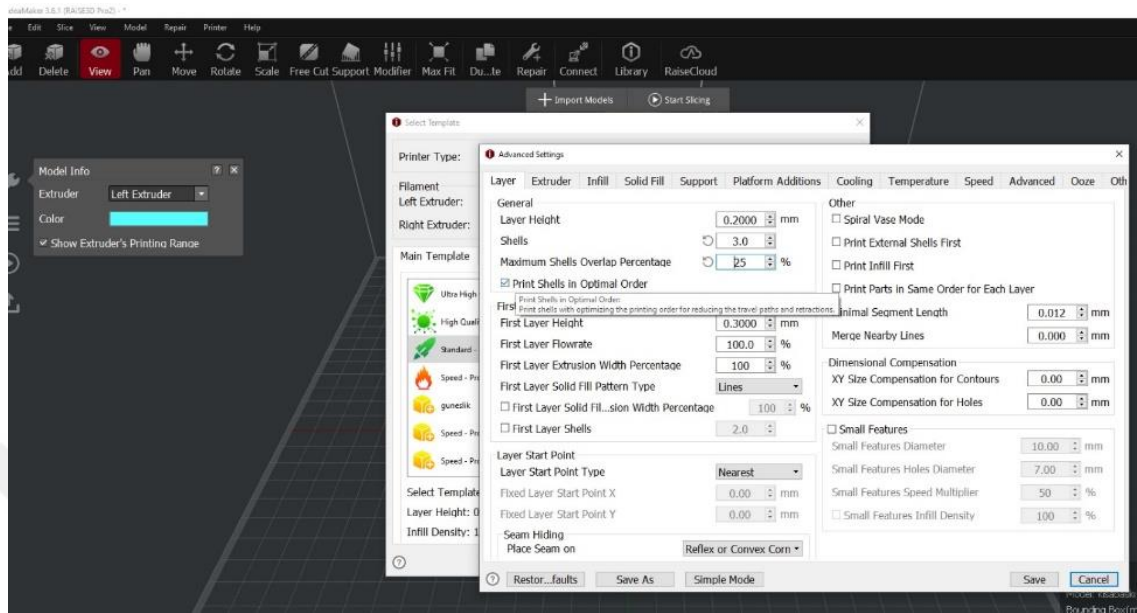


Figure 3.18 Shell number and shell crossing percentage

Shell number is defined as 3 and shell crossing as %25. Calculation of 1mm shell diameter is given in (Figure 3.20)

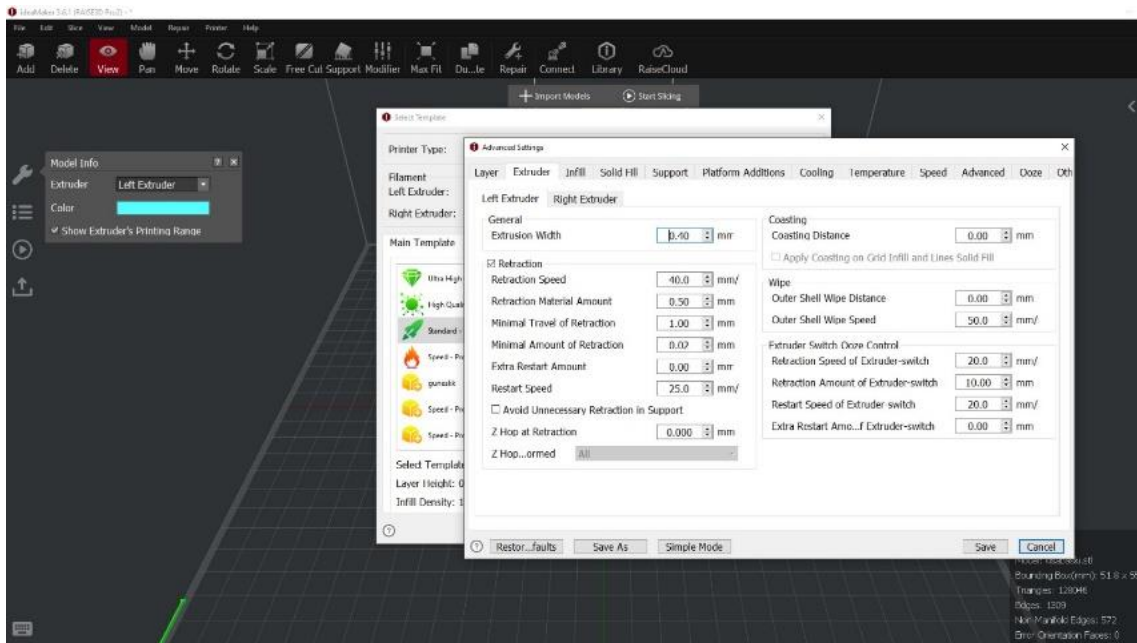


Figure 3.19 Extrusion width

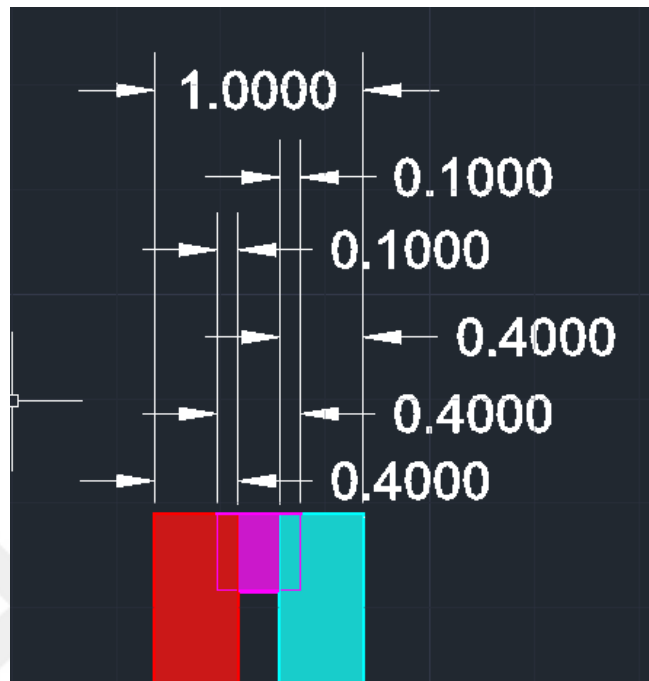


Figure 3.20 Shell diameter calculation

3.2.7 Printing of models

Main body of face shields and laryngoscopes 3D printed with Ultimaker 2+ 3D printer (Figure 3.21).

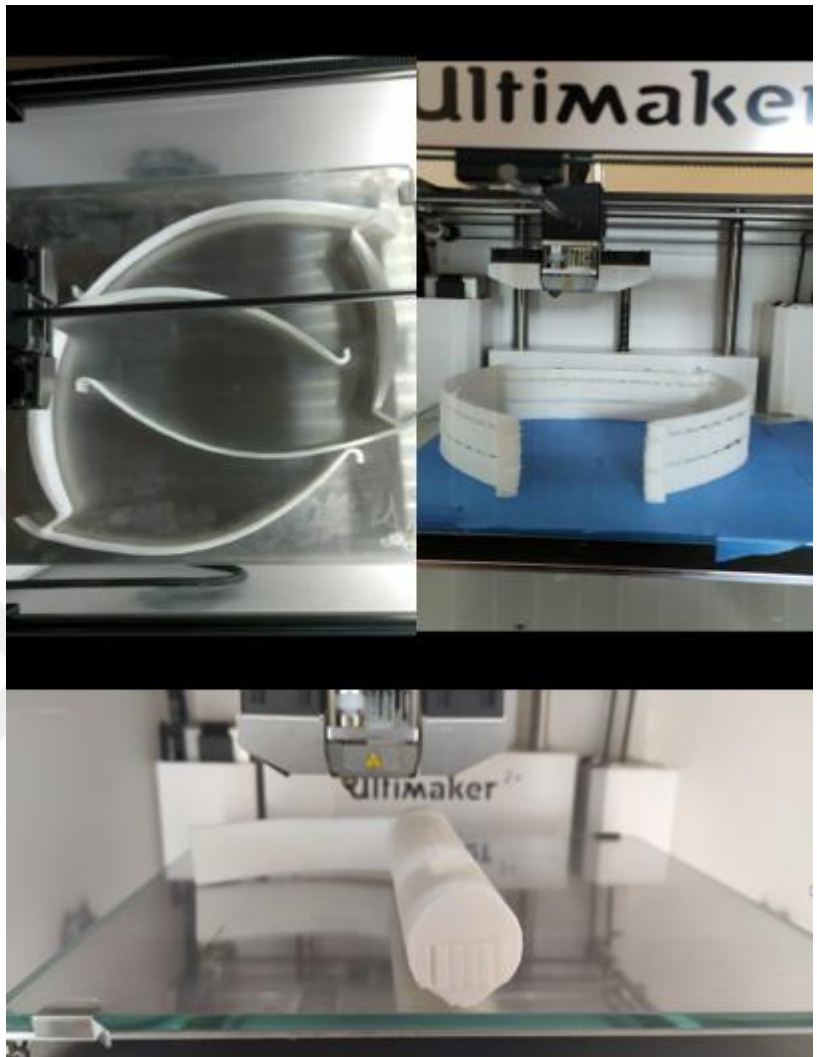


Figure 3.21 3D printing with Ultimaker 2+

Aorta samples 3D printed with Raise 3dpro 3D printer (Figure 3.22).

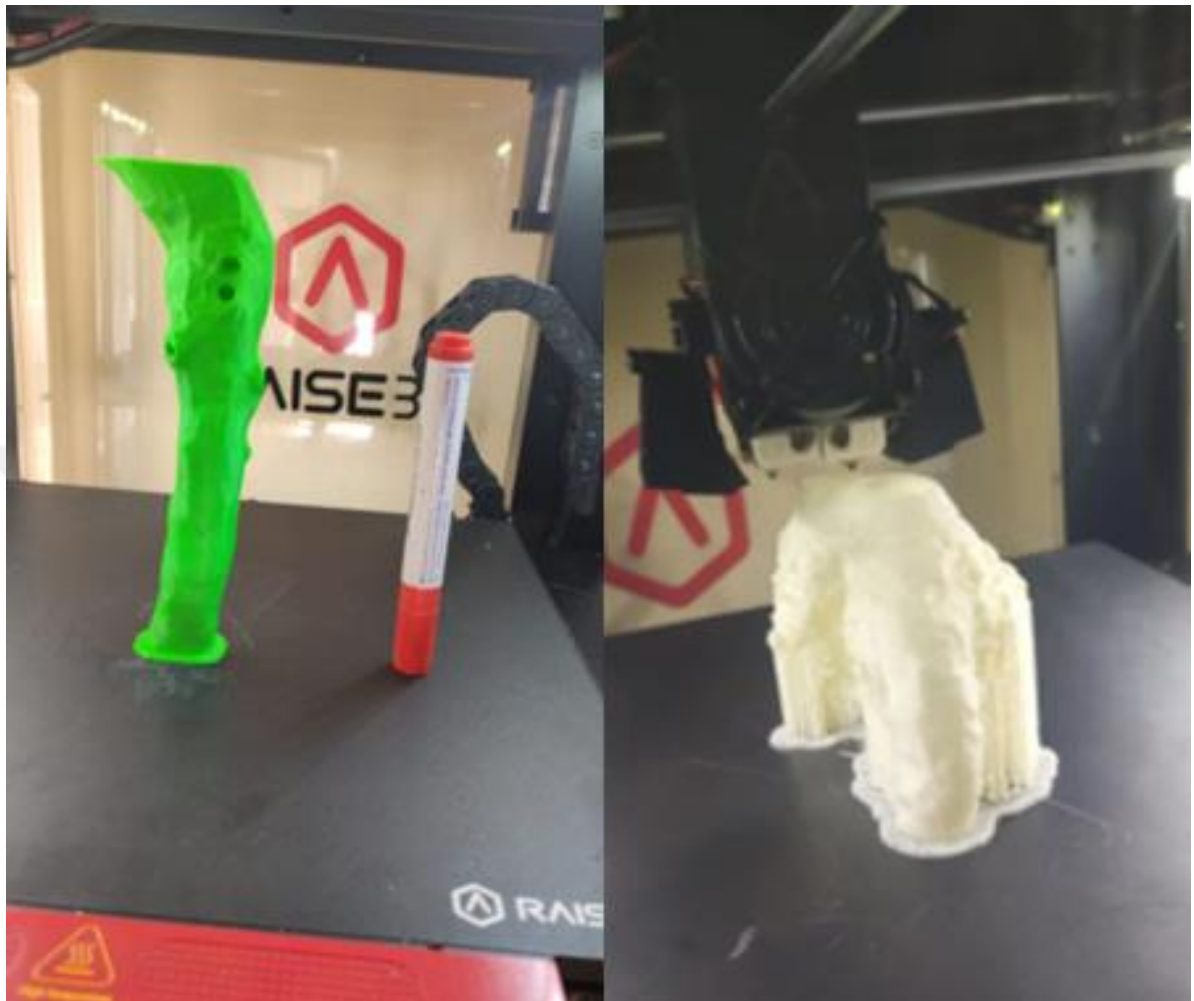


Figure 3.22 3D printing with Raise 3dpro

3.2.8 Post processing applications

Different post-processing applications are applied for each 3D printing. First of all, the main body of the face shield is combined with clamps, acetate paper, and elastic bands. The clamps are used for the attachment of acetate paper, and 3D printed main body of face shield as in (Figure 3.23).



Figure 3.23 Post-processing of face shields

An elastic band is used for the attachment of the face shield and human body as in (Figure 3.23). Only in the head covered model face shields elastic band is supported with an adjustable clamp, as well.

3.2.9 Compression strength characterization of 3D printed models

Compression strength characterization of 3D printed models tested with the universal testing machine of Shimadzu. The used device is the 10kN (kilo) (Newton) tabletop model given in (Figure 3.24).



Figure 3.24 Universal testing device

The compression strength of laryngoscopes was tested with a 5mm/min rate of compressing (Figure 3.25). Laryngoscopes positioning before the test is given in (Figure 3.26). Aorta's positioning before the test is given in (Figure 3.27).

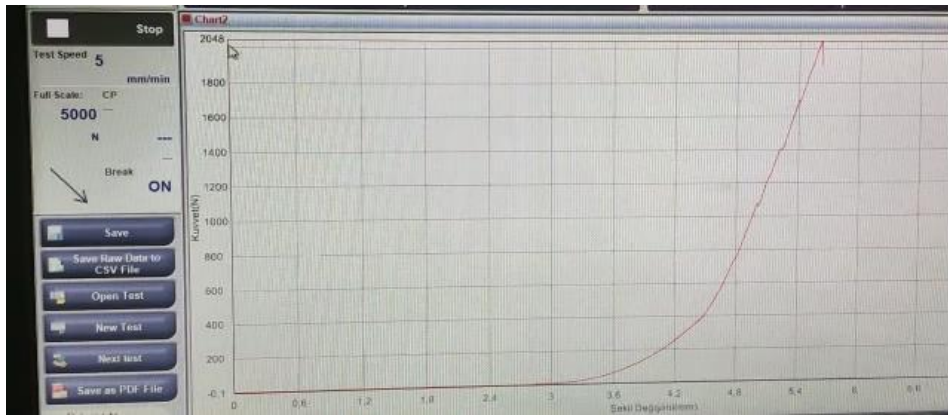


Figure 3.25 Compression stress test

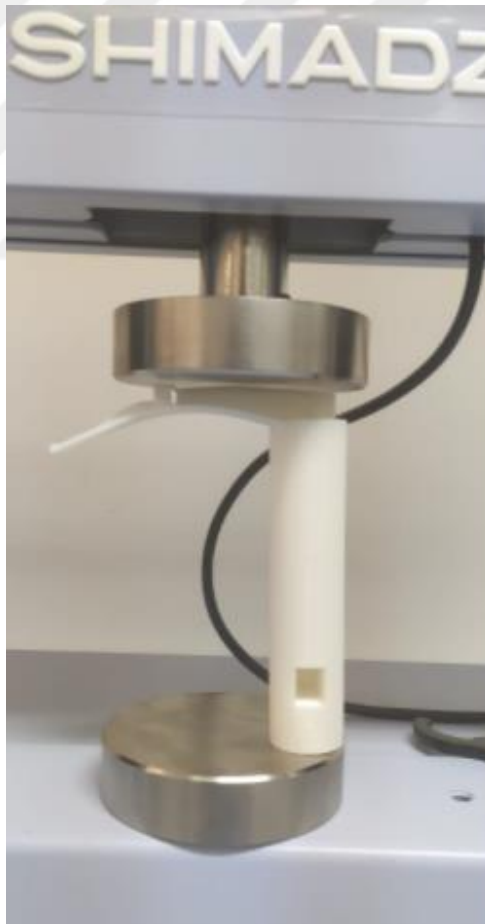


Figure 3.26 Compression test of laryngoscopes

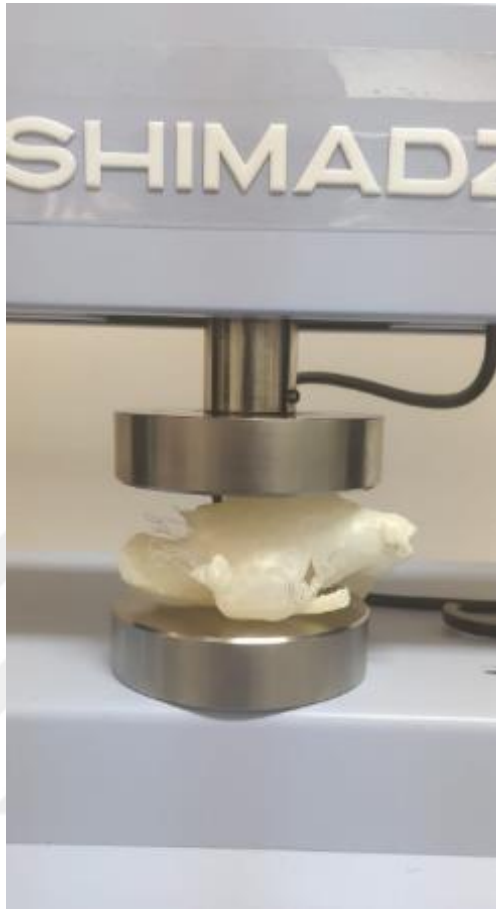


Figure 3.27 Compression test of aorta parts.

3.2.10 Tensile behavior characterization of 3D printed models

Tensile behavior of 3D printed models tested with the universal testing machine of Shimadzu. The used device is the 10kN tabletop model given in (Figure 3.24). Tensile strength of the aorta is tested with a 10mm/min rate of tensile movement (Figure 3.28).

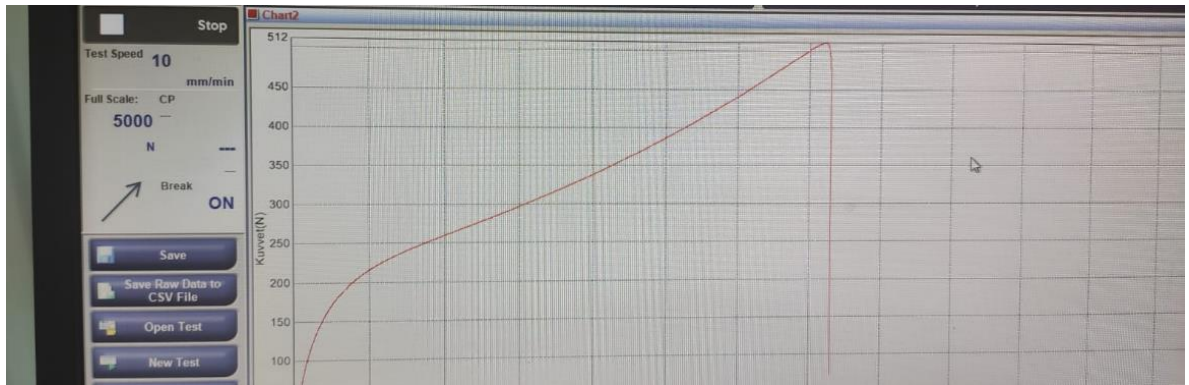


Figure 3.28 Tensile behavior test



Figure 3.29 Tensile behavior test of aorta parts

Since these test doesn't give reliable results a holder designed for tensile test (Figure 3.30).

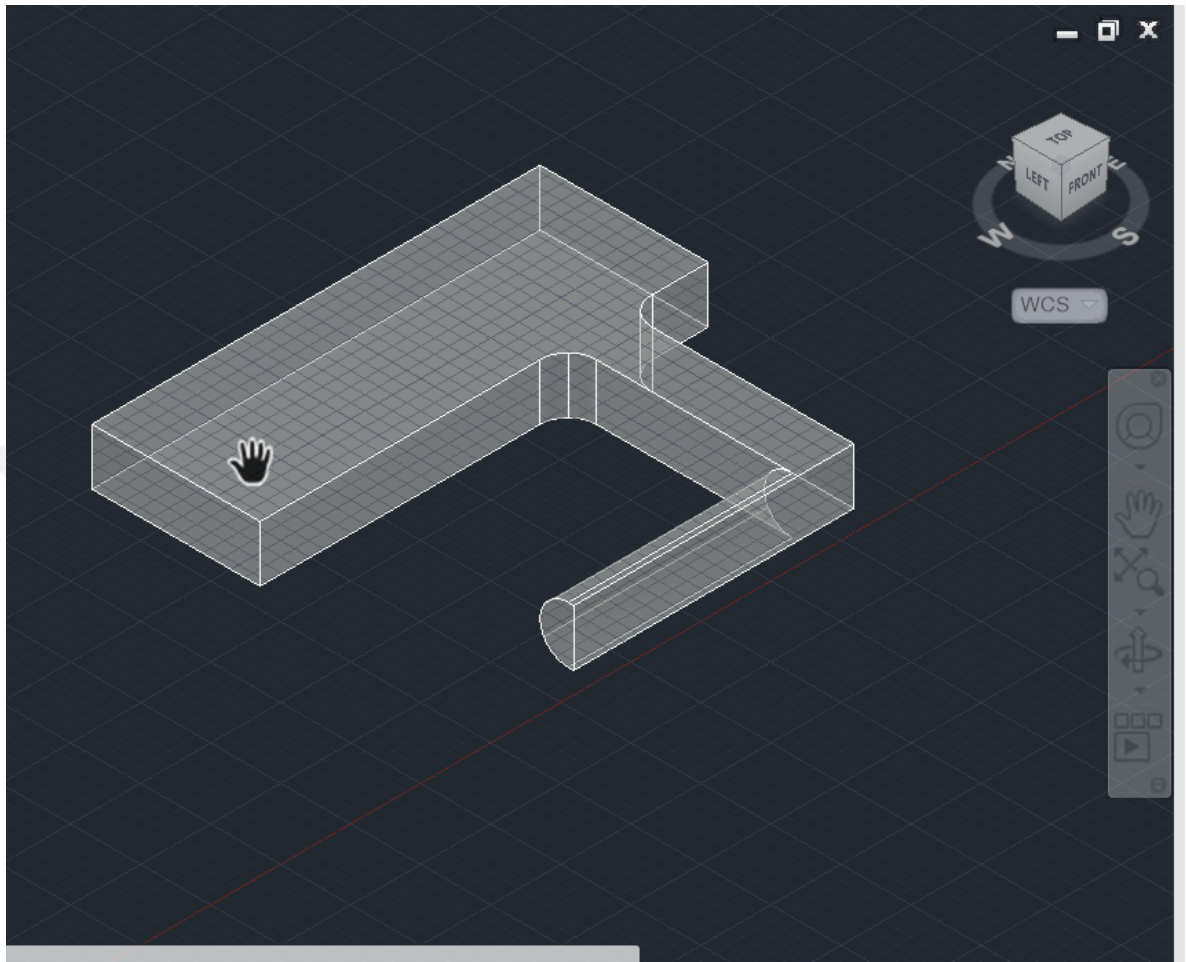


Figure 3.30 3D design of sample holder for tensile behavior test of aorta parts

This holder also 3D printed and used for tensile behaviour characterization of aortha parts. Aorta parts and samples positoning during test is given in (Figure 3.31).



Figure 3.31 Tensile behavior test of aorta parts with holder

3.2.11 Three point bending characterization of 3D printed models

Three point bending behavior of 3D printed models tested with universal testing machine of Shimadzu. Used device is 10kN table top model given in (Figure 3.24). Laryngoscopes head part is cut from total 3D model as in (Figure 3.32).

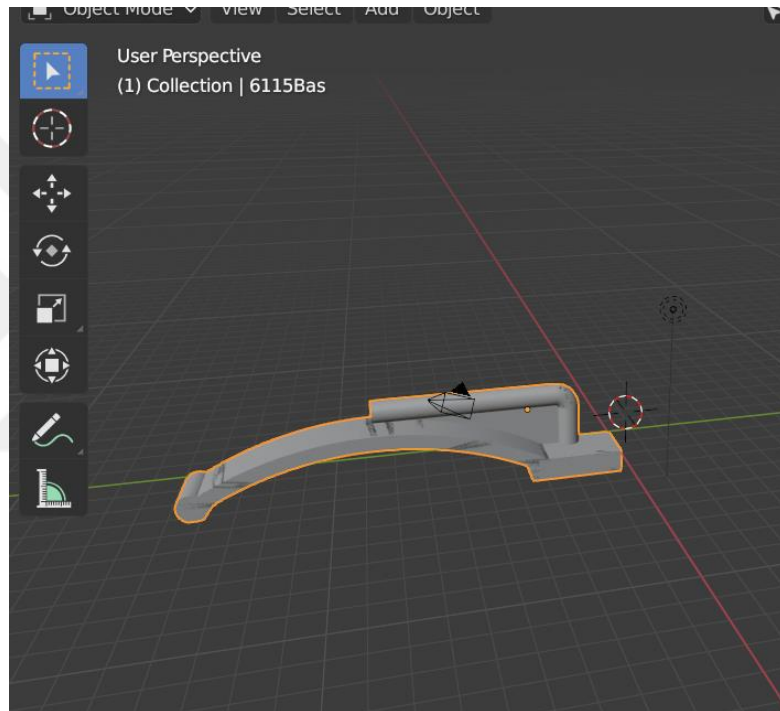


Figure 3.32 Design of head of laryngoscopes for three point bending test

3D printing of laryngoscopes head with different infill rate is given below. Samples positioning before test is given below.

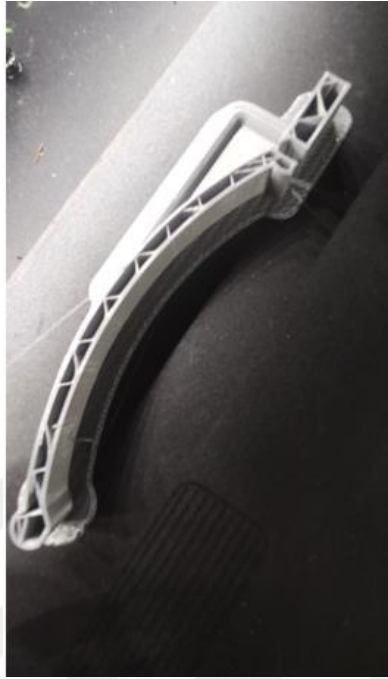


Figure 3.33 3D printing with 10% infill rate



Figure 3.34 3D printing with 25% infill rate

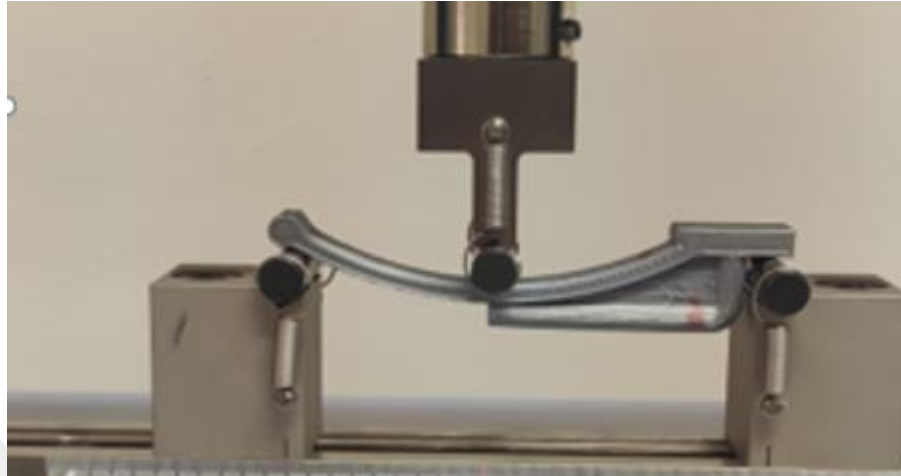


Figure 3.35 Three point bending test of 3D printed laryngoscope heads

3.2.12 Mechanical evaluation of Screws and Endobuttons for Latarjet Fixation Procedures

Screws and Endobuttons are evaluated for their mechanical properties using the universal testing machine of Shimadzu (Figure 3.24). Defect deciding of 3D printed scapula samples (Figure 3.36). Fixation of decided defects onto 3D printed scapula models in the anteroinferior of glenoid with screws (Figure 3.37). Fixation of decided defects onto 3D printed scapula models in the anteroinferior of glenoid with endobuttons (Figure 3.38).



Figure 3.36 Defect deciding



Figure 3.37 Fixation with endobuttons



Figure 3.38 Fixation with screws

A K wire (Kirschner Wire) is used in the tensile testing of screws and endobuttons (Figure 3.39).

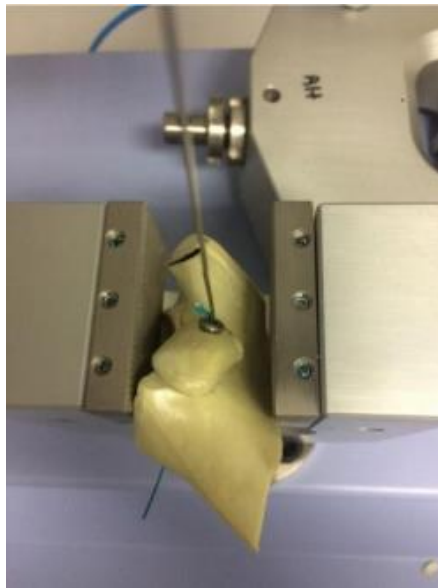


Figure 3.39 Tensile tests using K wire.

4. RESULTS AND DISCUSSION

4.1 Face Shields

During the main body design process of face shields, three different models were designed, which are the main body, reduced main body, and head covered main body. The reduced main body design was fast to 3D print, but the ergonomics of the design did not favor medical use hence this model was not produced in large quantities. Another design was head covered main body design it is produced as in (Figure 4.1).



Figure 4.1 3D printed head covered face shield

The chief physician office specially requested this design of hospitals of Ankara University in contrast to our previously given engineering advice which is it won't be applicable for 3D printing. Nevertheless, the design has been successfully manufactured as in the below Figure,

and as it can be easily seen, it is better in protection and ergonomic for continuous usage. However, the total printing of these models was about one day as in (Figure 4.2) for one sample; hence this model did not manufactured any other than its prototype.



Figure 4.2 3D printing procedure time of head covered main body

Last design was main body design it is produced as in (Figure 4.3).



Figure 4.3 3D printed face shield

This simple model is produced for more than one thousand and used in the fight against Covid-19. Only to “Türk Plastik Rekonstrüktif ve Estetik Cerrahi Derneği” one thousand of these models supplied. The printed forms of a small portion of them given in (Figure 4.4 and Figure 4.5).



Figure 4.4 3D printed face shields in the help fight against Covid19.



Figure 4.5 3D Printed face shields in the help fight against Covid19

4.2 Laryngoscopes

4.2.1 Simulation of laryngoscope designs

Several laryngoscope designs were possible according to the commercially available laryngoscope model in (Figure 3.7). Parts of the suggested model are mentioned in the methods part thoroughly. The blue labeled part in (Figure 3.8) is the central angled part of laryngoscopes. Hence it is the weakest part of or, in other words, the central load-bearing part of the design. To understand the force distribution in this part laryngoscope model is analyzed in the simulation mode of Autodesk's Inventor cam/cad program. During these simulations thickness of the angled part and the angle is changed to optimize the design for better load-bearing ability. The circle's diameter characterizes the angle of the angled part during the simulations processes of 100N, 200N, and 400N of force applied to the model. 200N, which can be thought of as 20kg (kilogram) of force, is pre-assumed as the maximum force can be generated by the medical professionals during intubating process. This 20kg value is found by simply pushing through a scaler as much as a human body can. Moreover, half of this value and double of this value are simulated to optimize the force distribution better. After the simulation scale bar of stress, the max is, which is red, decided as 80 MPa (Mega) (Pascal), to keep the 59MPa which is the ultimate stress value PLA samples, in the top of the green region (Oosthuizen, Hagedorn-Hansen et al. 2013). Finally, if the stress distribution in simulated design is colored in all blue or blue and the green sample passes if it includes any yellow or red part, it fails.

Evaluation of 3mm thickness and radius of 115mm Samples

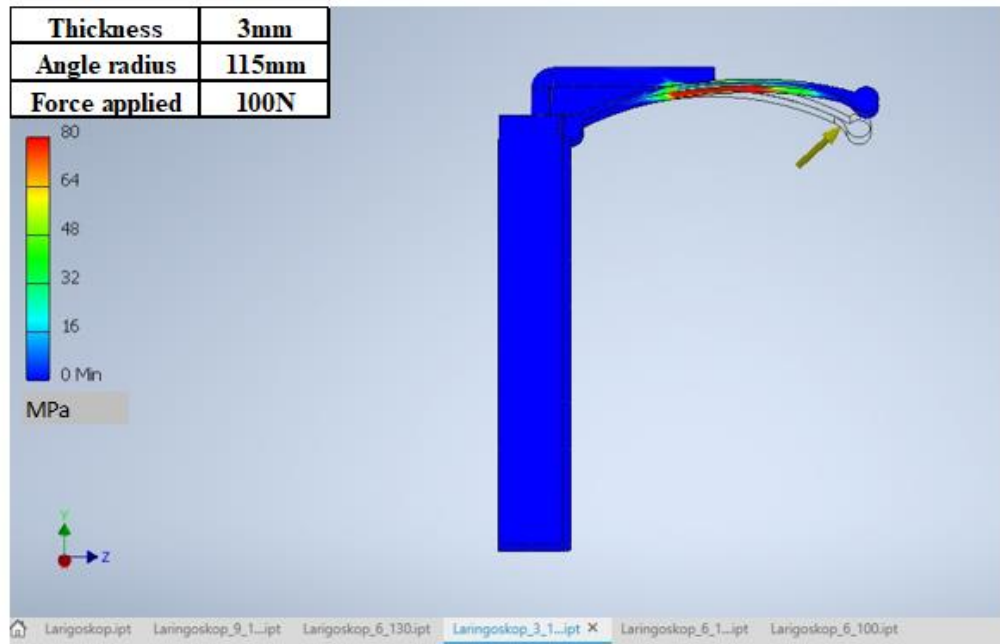


Figure 4.6 3mm (mili meter) thickness and radius of 115mm sample under 100N force

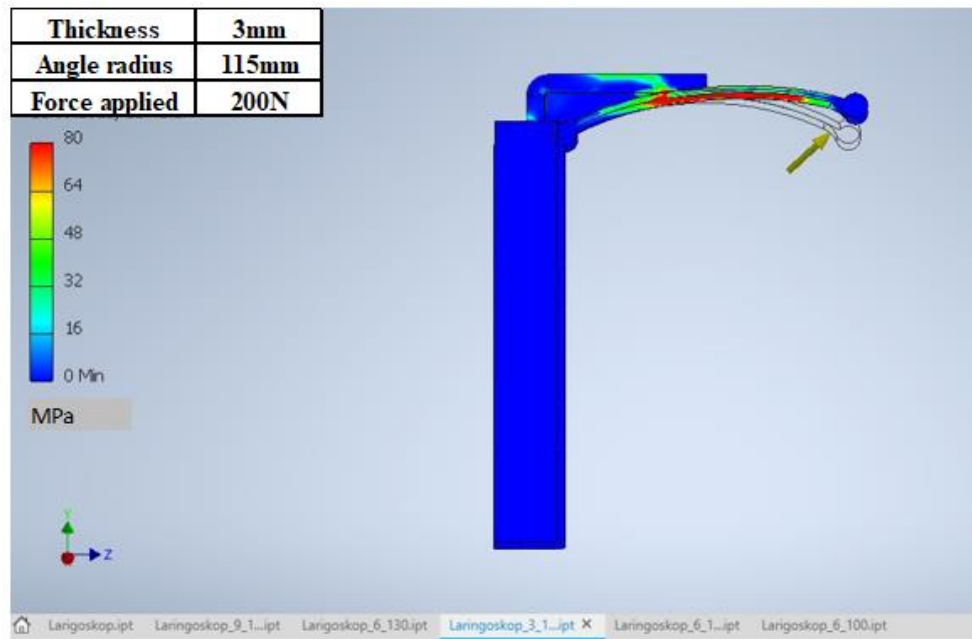


Figure 4.7 3mm thickness and radius of 115mm sample under 200N force

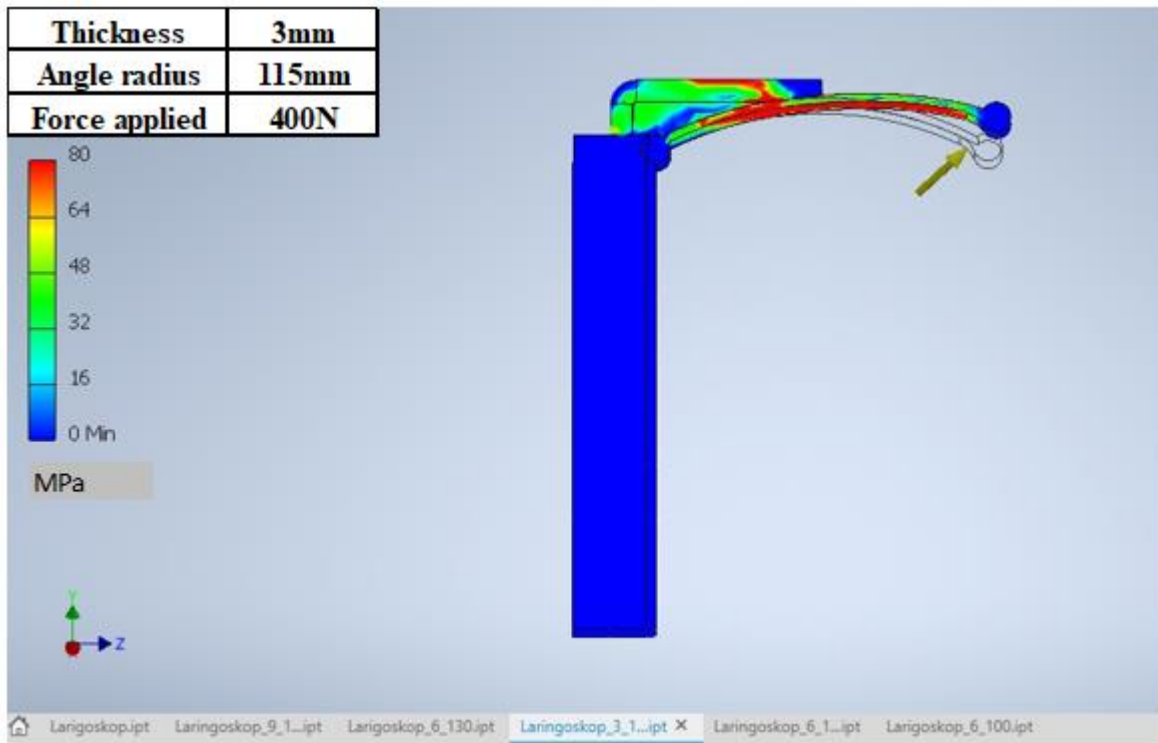


Figure 4.8 3mm thickness and radius of 115mm sample under 400N force,

As can be seen from the (Figure 4.6-8) 3mm thickness of samples failed in all of the subjected forces. So 3mm thickness was found as not suitable and the studied thickness increased to 9 mm.

Evaluation of 9mm thickness and radius of 115mm Samples

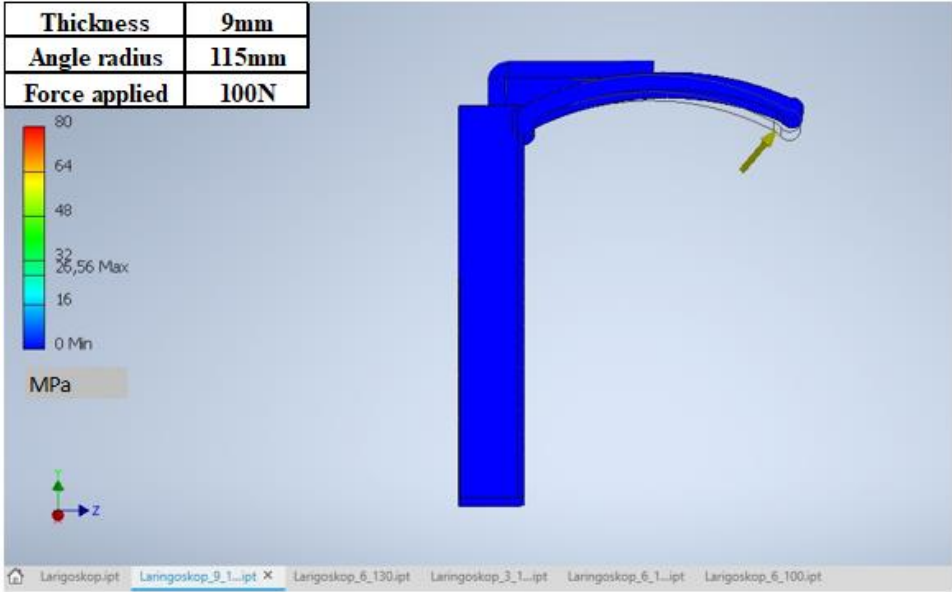


Figure 4.9 9mm thickness and radius of 115mm sample under 100N force

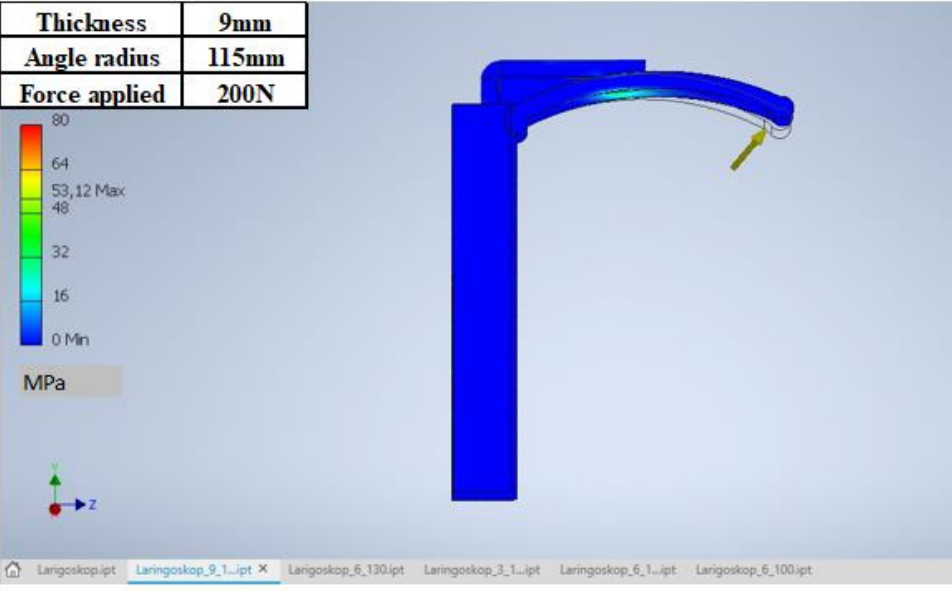


Figure 4.10 9mm thickness and radius of 115mm sample under 200N force

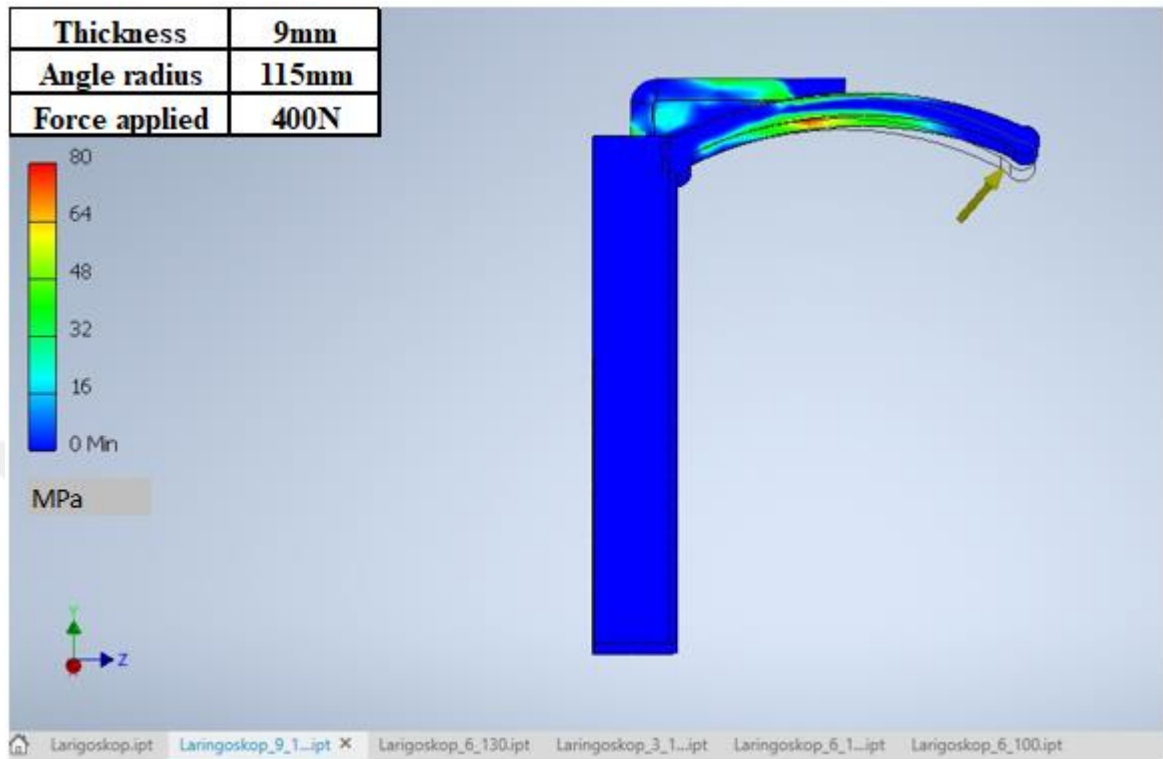


Figure 4.11 9mm thickness and radius of 115mm sample under 400N force

As can be seen from (Figures 4.9 and 10), 9mm thickness of samples was succeeded in 100N and 200N of the subjected forces. But 9mm thickness was found as not suitable for 400N of force. Since 40kg of force is to be generated during the intubation highly unlikely, and 9mm succeeded 200N force simulation thickness is reduced to 6mm.

Evaluation of 6mm thickness and radius of 115mm Samples

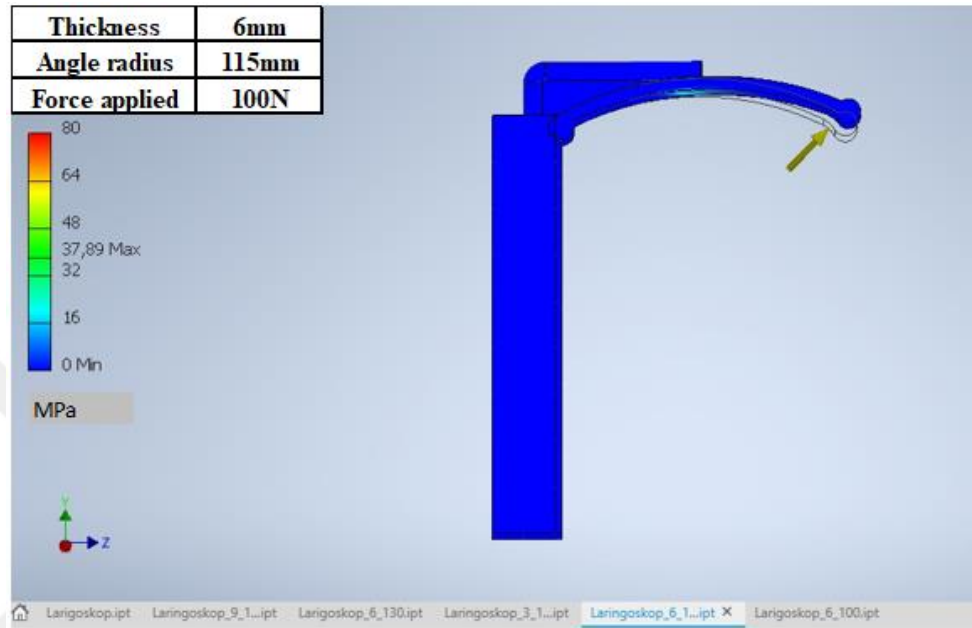


Figure 4.12 6mm thickness and radius of 115mm sample under 100N force

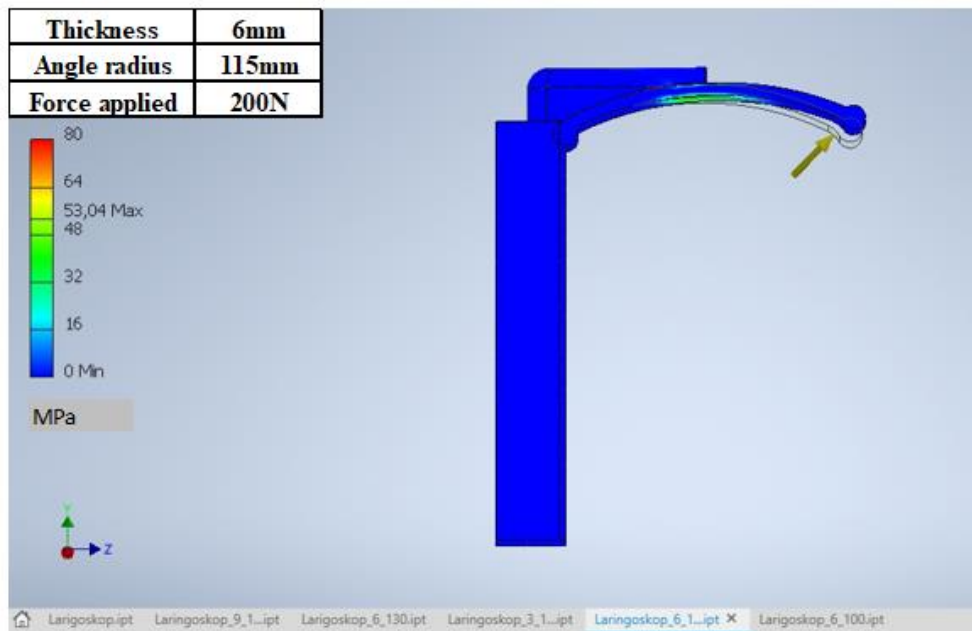


Figure 4.13 6mm thickness and radius of 115mm sample under 200N force

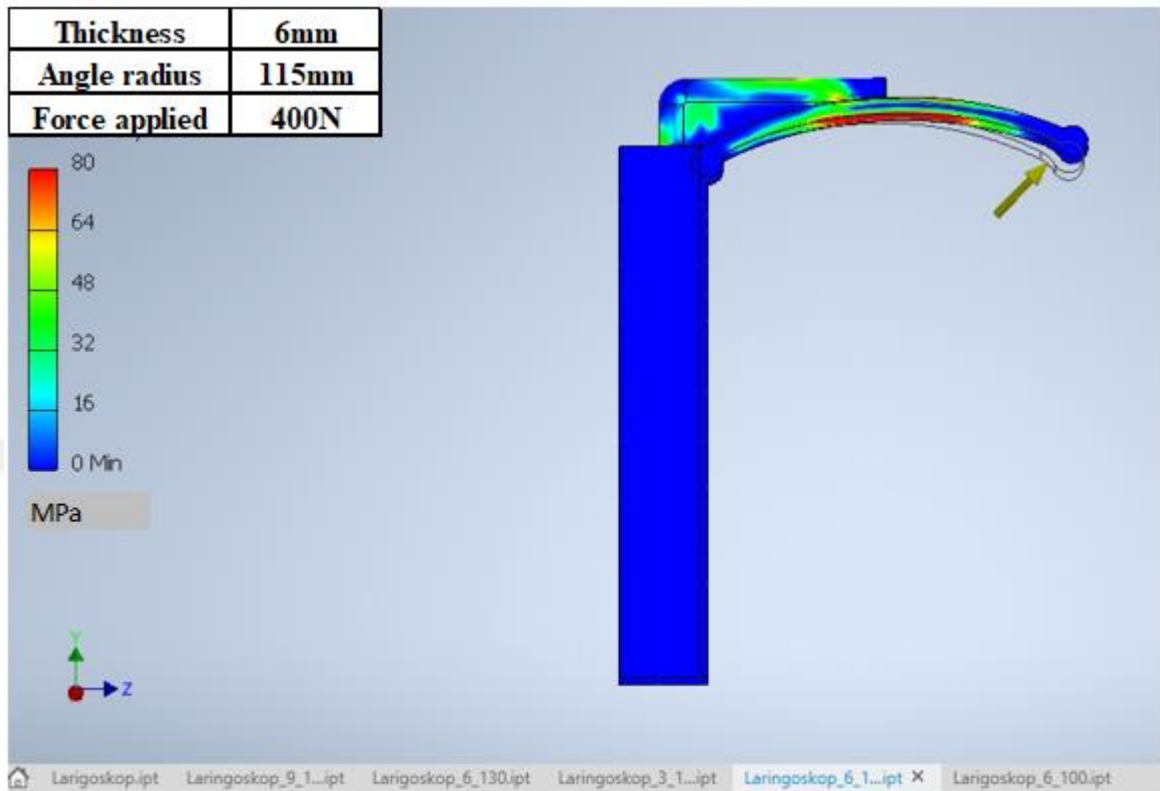


Figure 4.14 6mm thickness and radius of 115mm sample under 400N force

As in (Figure 4.11 and Figure 4.14), the sample with 6 mm diameter still failed as 9mm diameter under 400N of force. Although it was successful as a 9mm diametric sample under 100N and 200N, as can be easily seen from (Figure 4.12 and Figure 4.13) whose do not include any yellow or red stress distribution. Moreover, 6mm of diameter is decided for the diameter of the angled part of the laryngoscopes design. After that, Evaluation of angle is needed for better optimization of design parameters.

Evaluation of 6mm thickness and radius of 100mm Samples

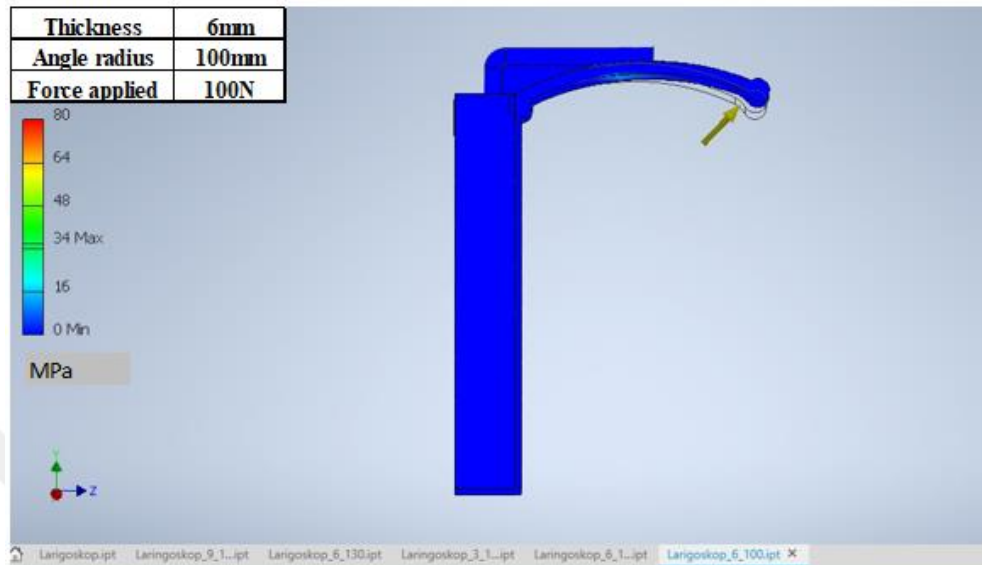


Figure 4.15 6mm thickness and radius of 100mm sample under 100N force

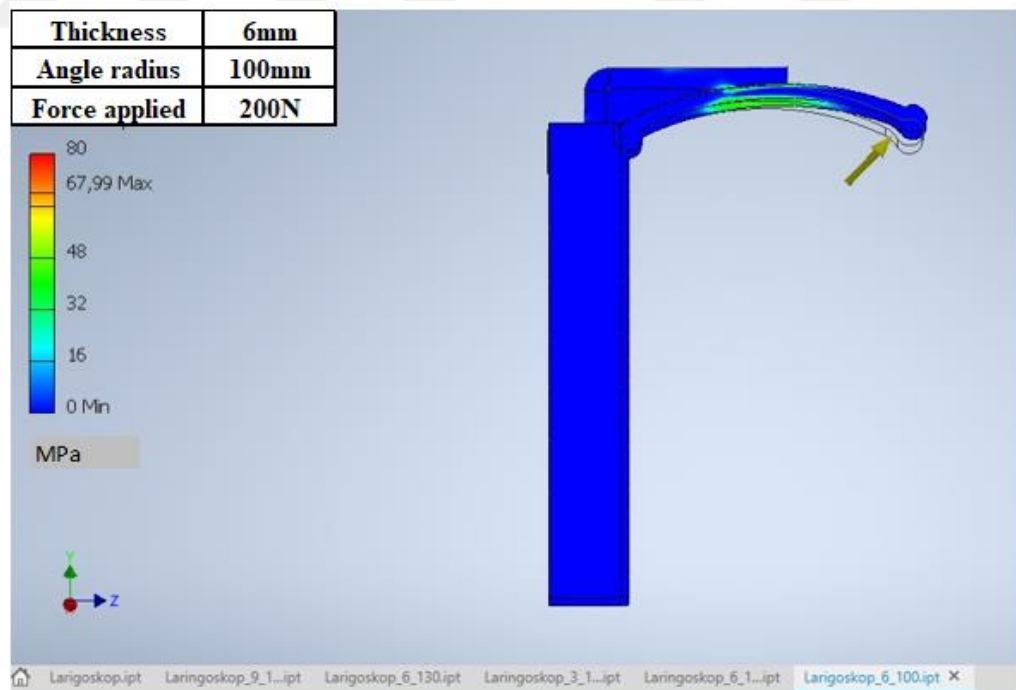


Figure 4.16 6mm thickness and radius of 100mm sample under 200N force

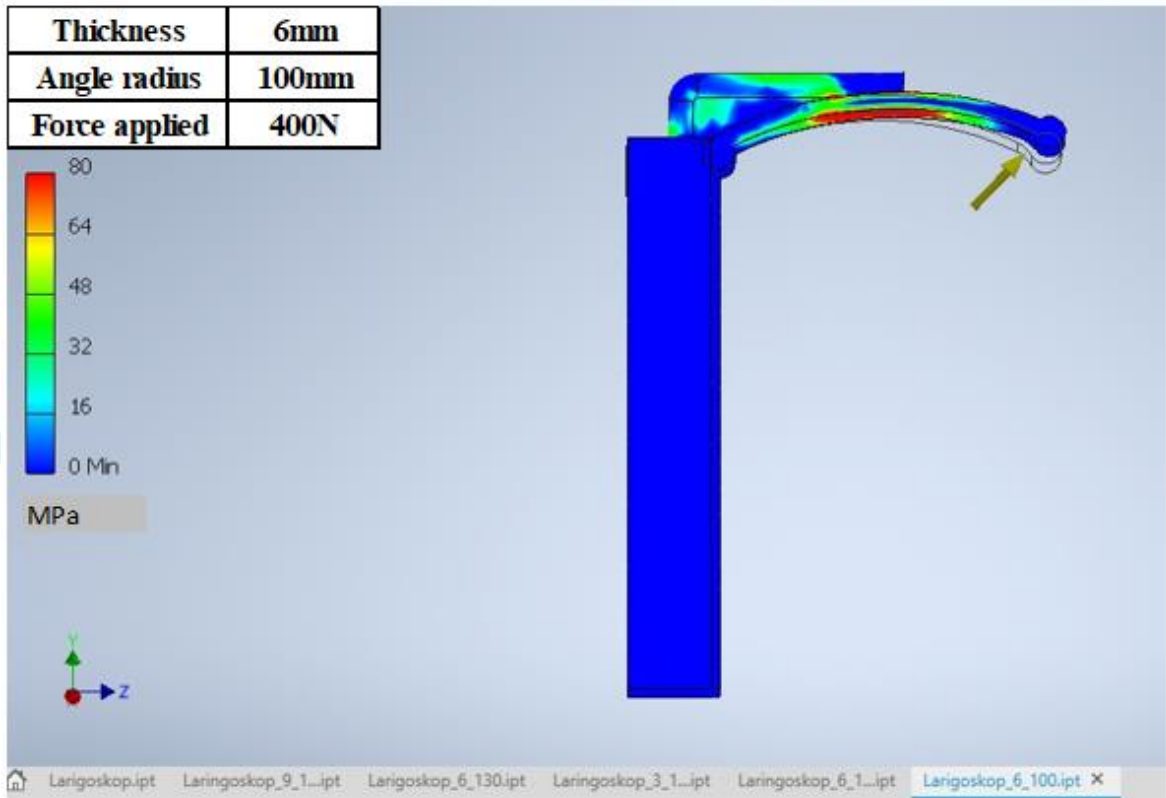


Figure 4.17 6mm thickness and radius of 100mm sample under 400N force

As shown from (Figure 4.15-17), only 6mm diameter and 100mm radius configuration is succeeded under 100N and failed under 200N and 400N. Hence it is not suitable. We continued with the 115mm radius of angle, and it was successful, as mentioned before.

Evaluation of 6mm thickness and radius of 130mm Samples

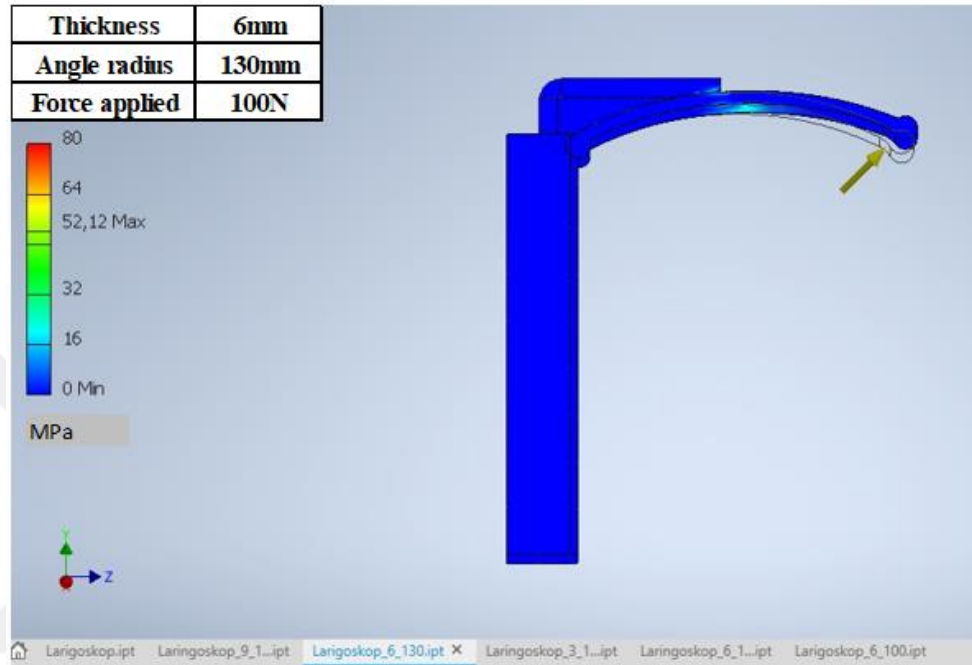


Figure 4.18 6mm thickness and radius of 130mm sample under 100N force

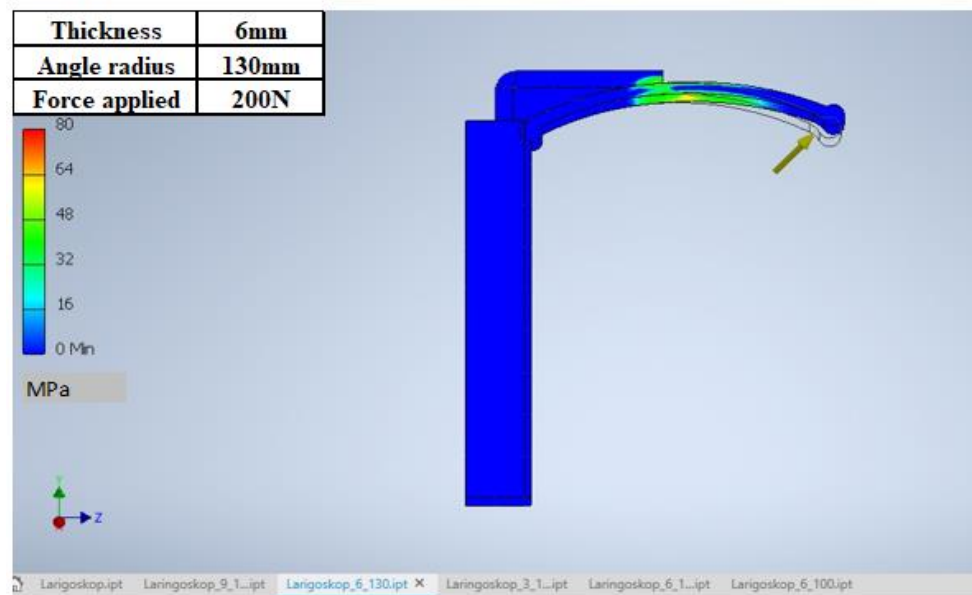


Figure 4.19 6mm thickness and radius of 130mm sample under 200N force

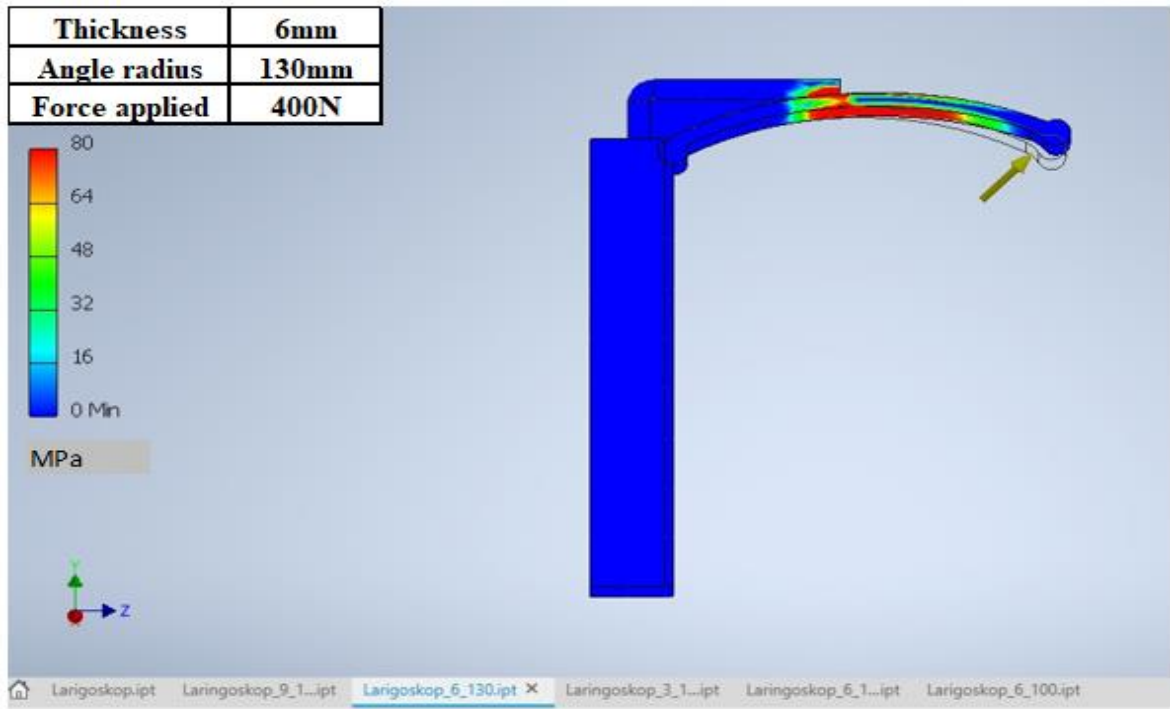


Figure 4.20 6mm thickness and radius of 130mm sample under 400N force

As can be seen from (Figure 4.18-20), samples with 130 mm radius both failed under 200N and 400N of applied force. Moreover, these samples are subjected to up to 52.12 MPa of stress generation under 100N of applied force. Since it is to near to our critical stress value, which is 59 MPa, it would be very risky to use this configuration.



Figure 4.21 Summary of Simulations

In conclusion, many thickness values and angle value is tried for optimization of angle. This optimization process actually consisted of many parameter changes and a mixed form of angle and thickness values (Figure 4.21). This optimization process is given in here in an organized form of thickness and angle optimization, respectively.

Finally design with 6mm and angle radius of 115m is found as best candidate for laryngoscope design and experiments are continued with this design.

4.2.2 Evaluation of laryngoscopes under compressive stress

While we were planning to characterize laryngoscopes mechanically, the compression test was the first experiment that came to our mind. However, during the experiments, as you can see in (Figure 3.26), it seemed impossible to standardize the force and stress-related. Moreover, during the simulations process, we have seen that maximum stress value occurs at the middle point of the bending curve with the applied force. Thus, it seemed more convenient and appropriate to mechanically characterize the laryngoscopes with a three-point bending test. As a result, we have added the evaluation of laryngoscopes with three point bending test into our experiments.

4.2.3 Evaluation of laryngoscopes with three point bending test

Final design according to simulation results was the design with 6mm and angle radius of 115m. This design is printed with 10, 25, 50, 75 and 100 % infill rates in order to decide which is most optimal. Young Modulus' of different infill rates are given in (Figure 4.22).

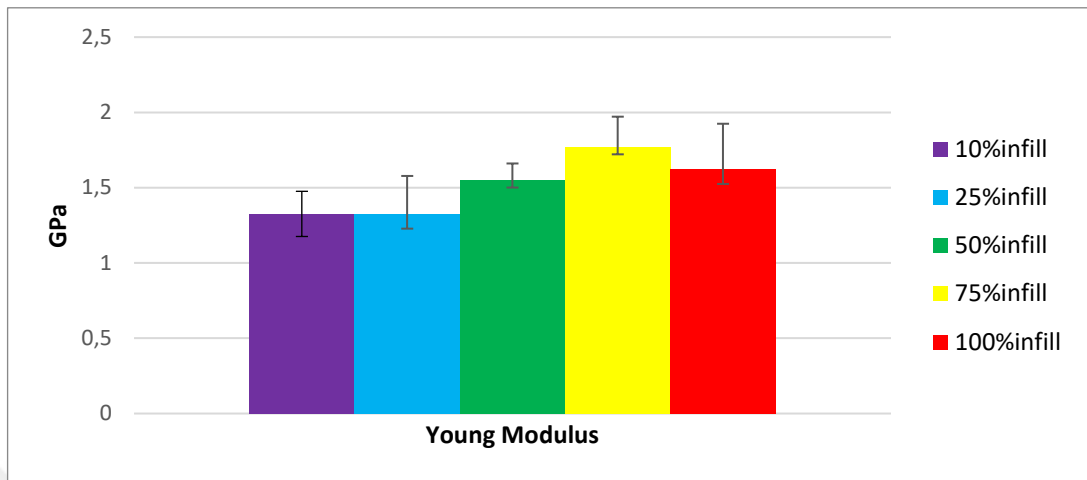


Figure 4.22 Young modulus of laryngoscope head with different infill rates

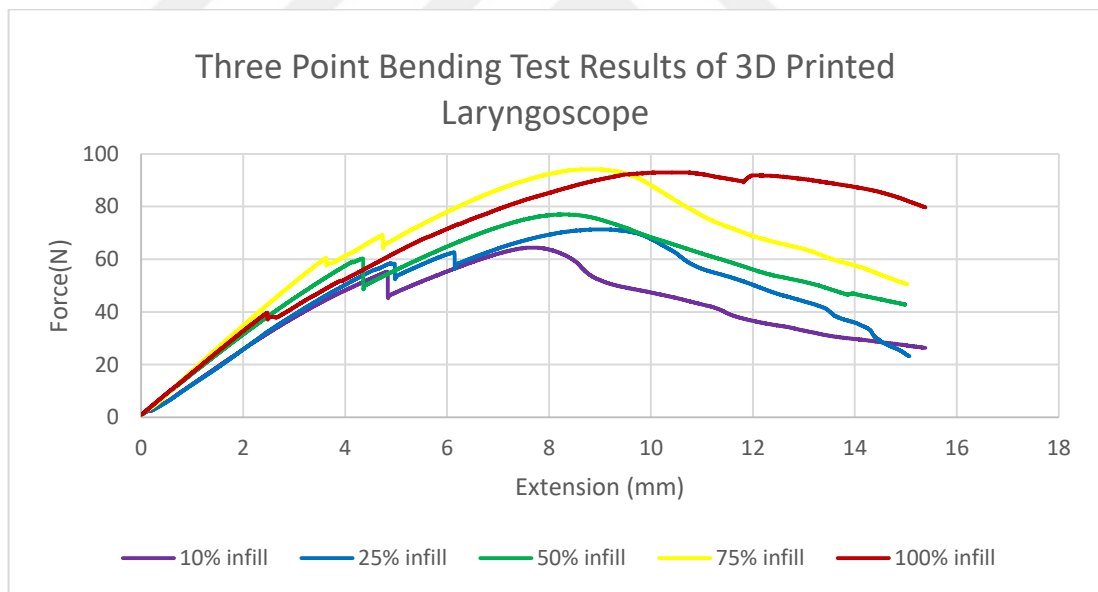


Figure 4.23 Three Point Bending Test Results of 3D Printed Laryngoscope

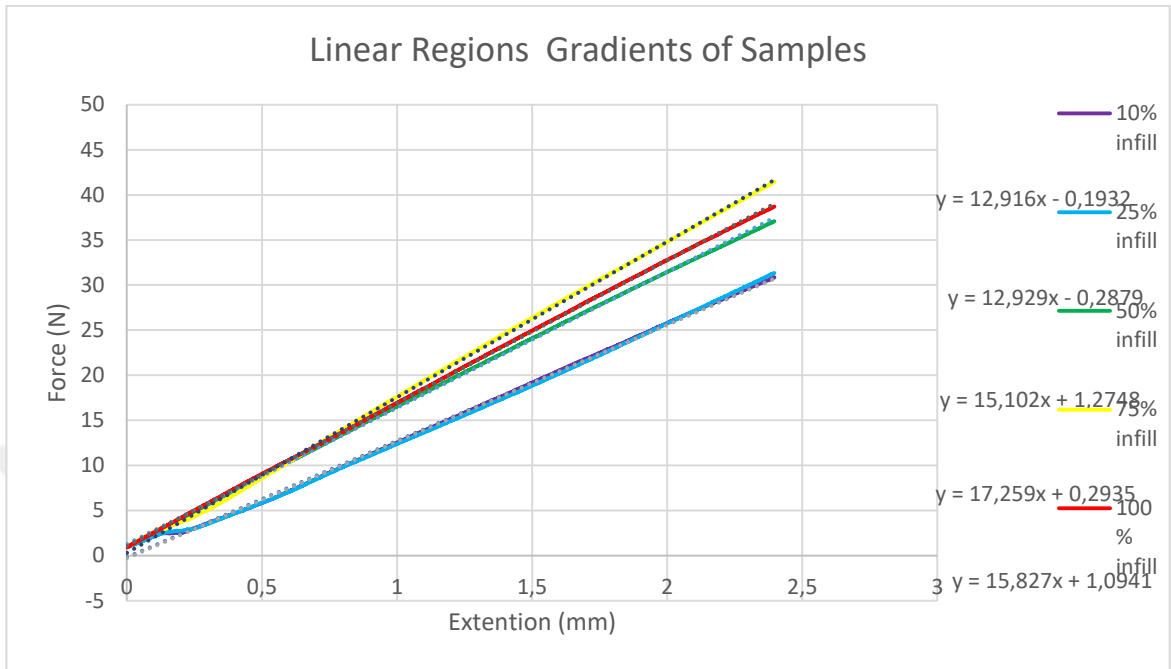


Figure 4. 24 Linear region of Three Point Bending Test Results of 3D Printed Laryngoscope

Pictures of laryngoscope heads before, after, and during the experiments given in respectively (Figures 4.25-27).

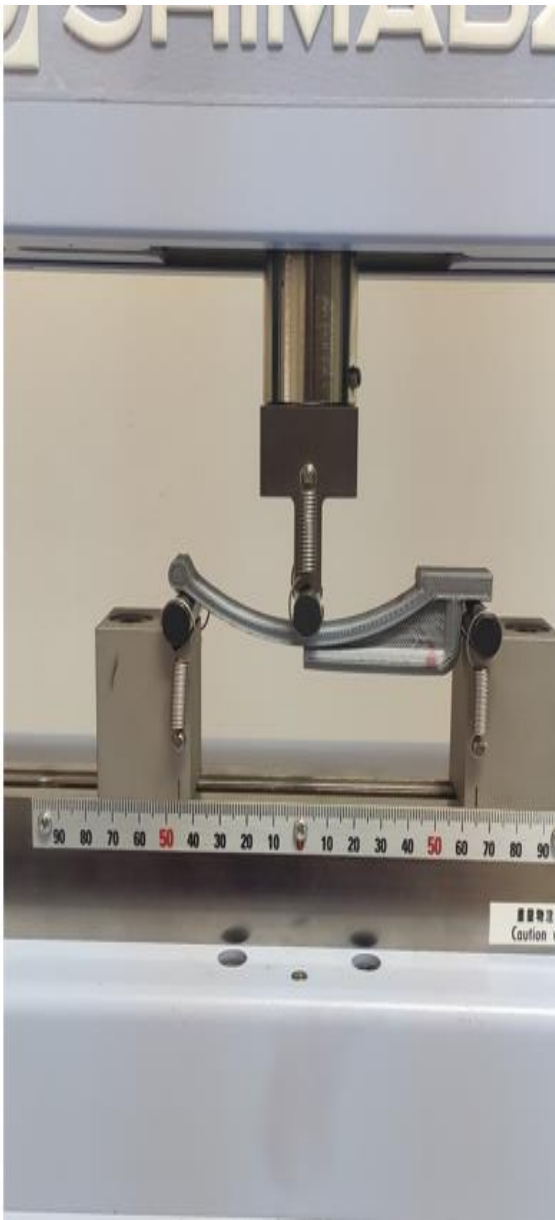


Figure 4.25 Samples before three point bending



Figure 4.26 Samples after three point bending

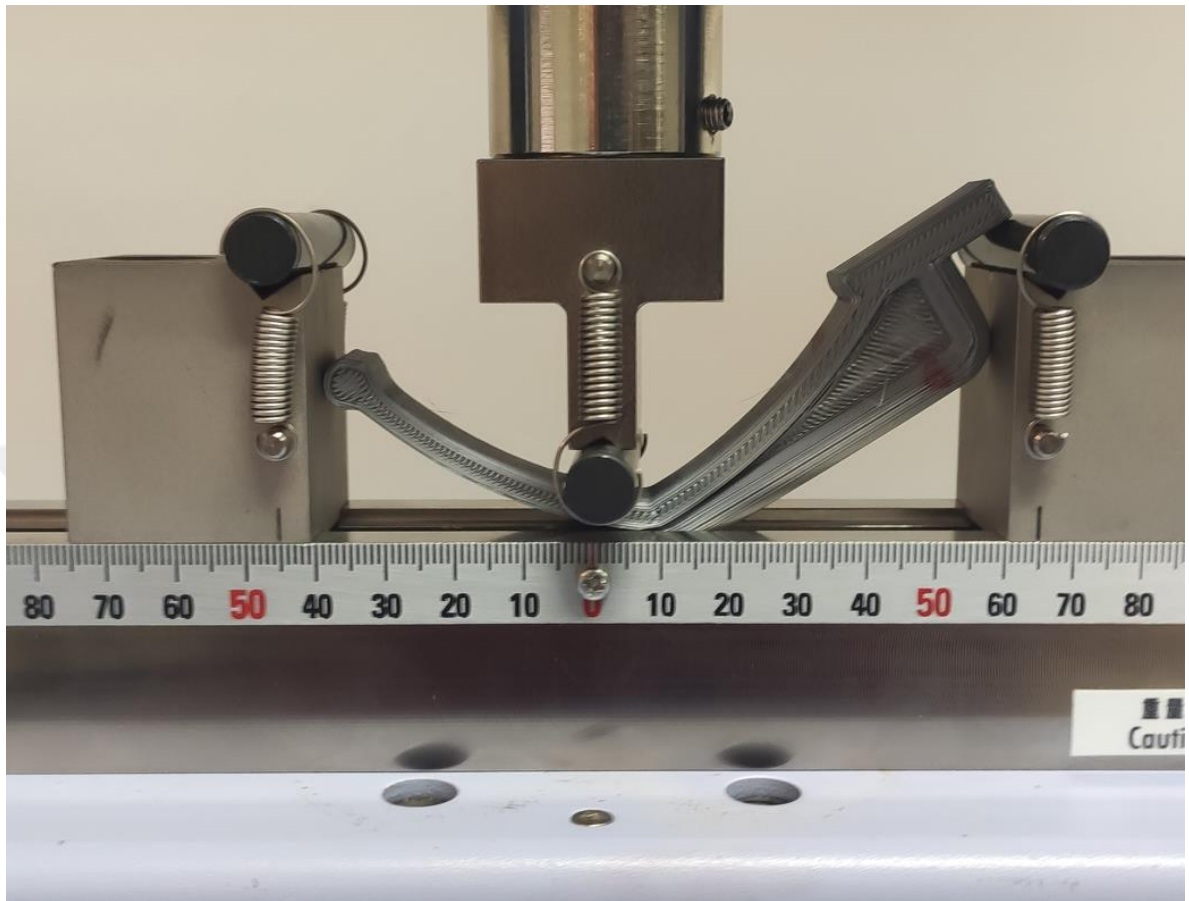


Figure 4.27 Samples during three-point bending

After characterization of different model it is found that 50, 75, 100 % of infills shows better mechanical property than 10 and 25 %. Since mechanical properties of 50 and 100% are similar, samples printed with 50 % infill for both time and material preservation.

4.3 Evaluation of Screws and Endobuttons

Endobuttons can be accepted as less aerosol creating methods in the Latarjet fixation methods when comparing with the screws because they reduce the steps of the surgery. In this part of the thesis, this type of fixation is evaluated in view of mechanical properties to understand whether this is better or equals for each other.

4.3.1 Evaluation of screws under tensile stress

Three samples of 3D printed scapula and a defect gathered from the scapula implanted into scapula itself with screws evaluated with tensile tests. Stress-Strain curves of the samples given (Figures 4. 28-31).

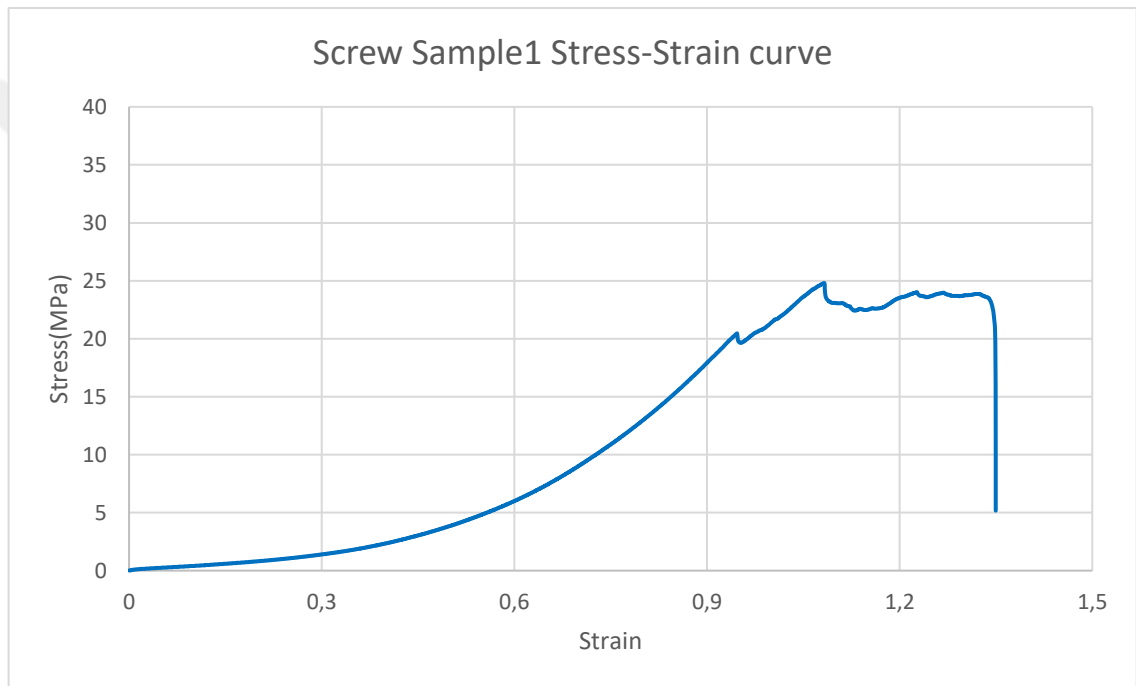


Figure 4. 28 Tensile behavior characterization of Screw Sample1

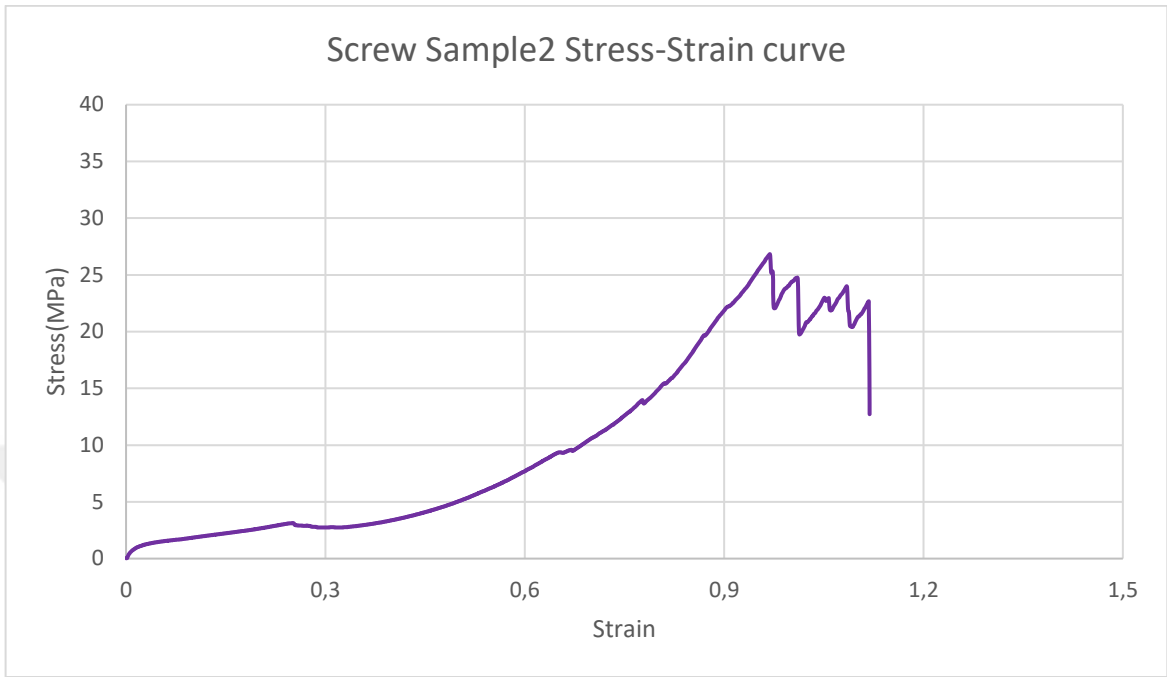


Figure 4.29 Tensile behavior characterization of Screw Sample2

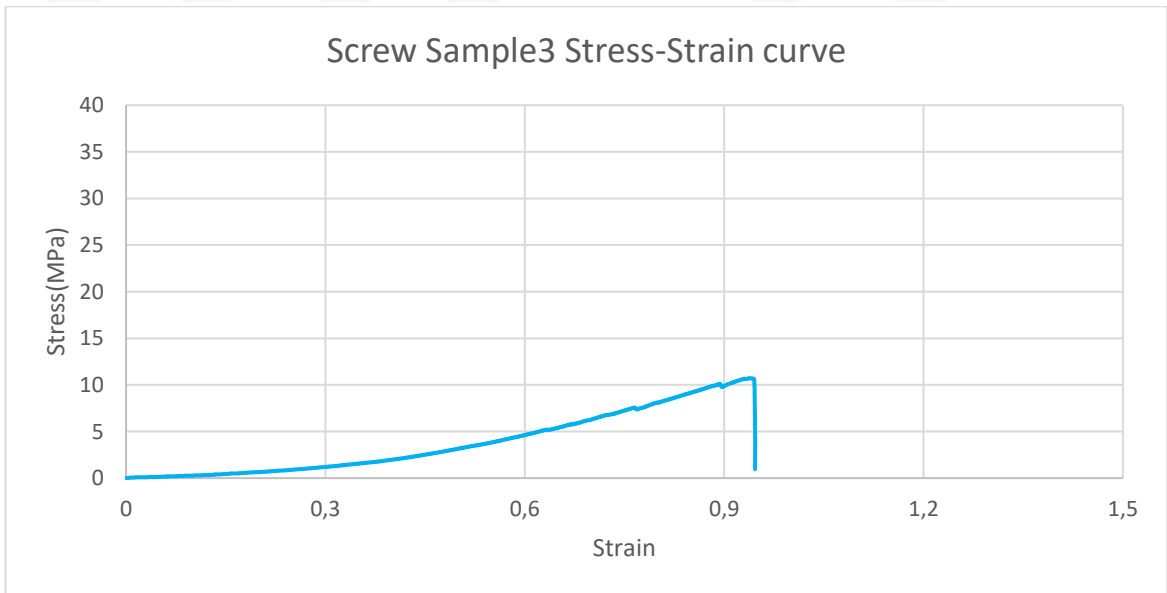


Figure 4.30 Tensile behavior characterization of Screw Sample3

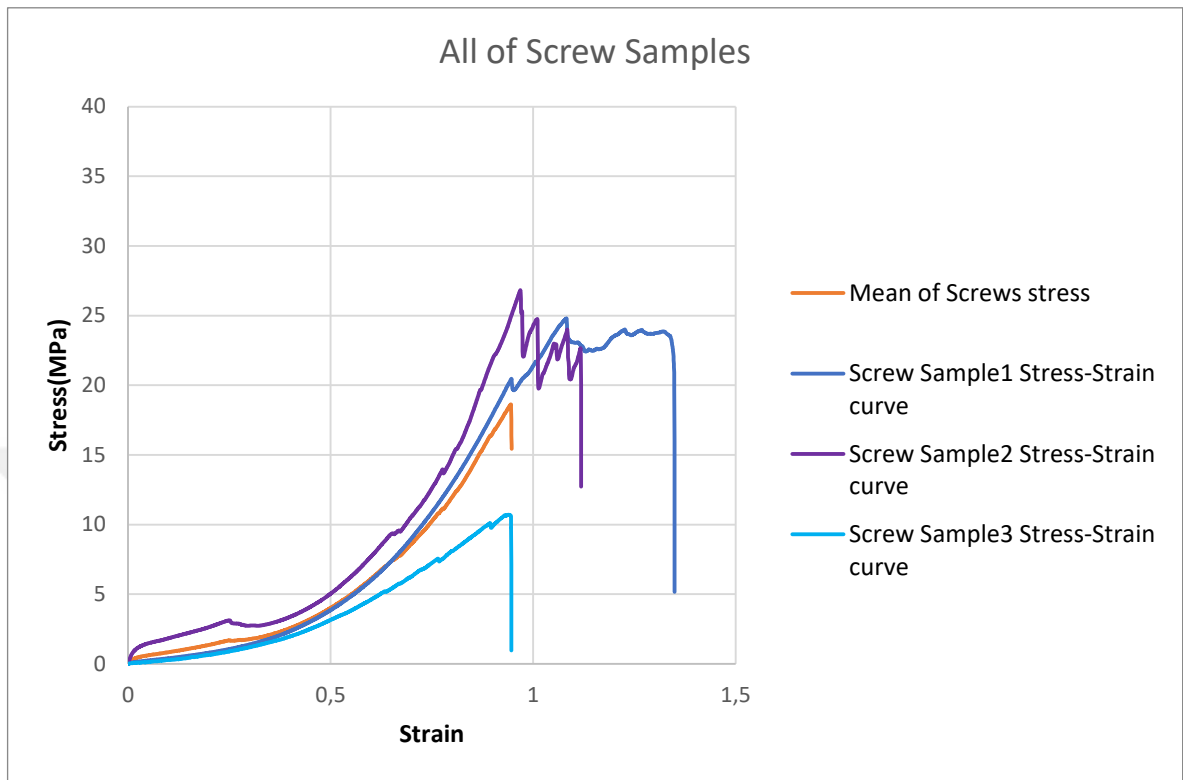


Figure 4.31 Tensile behavior characterization of Screw Samples

4.3.2 Evaluation of Endobuttons under tensile stress

Three samples of 3D printed scapula and a defect gathered from the scapula implanted into scapula itself with endobuttons evaluated with tensile tests. Stress-Strain curves of the samples given in (Figures 4. 32-35).

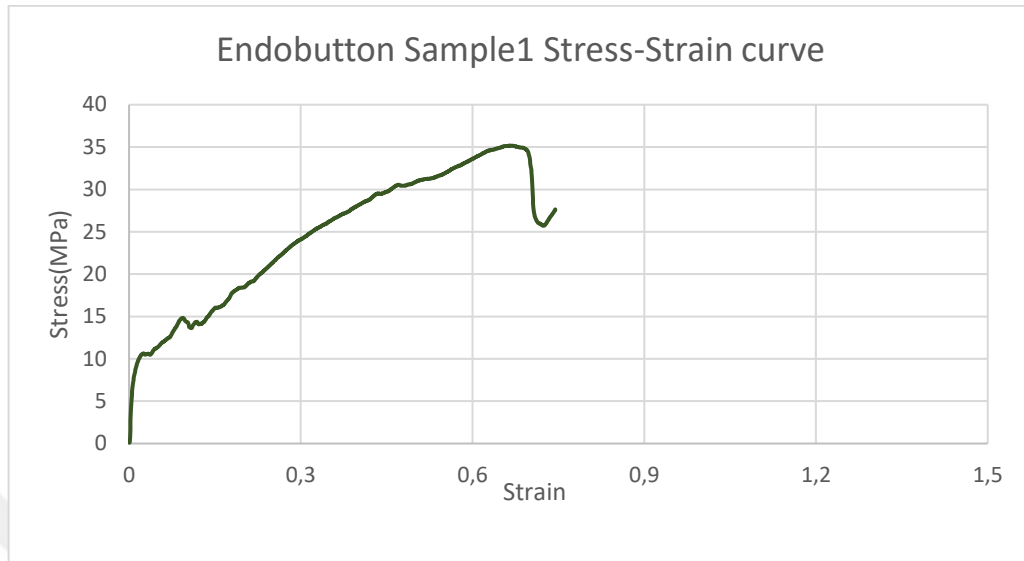


Figure 4.32 Tensile behavior characterization of Endobutton Sample1

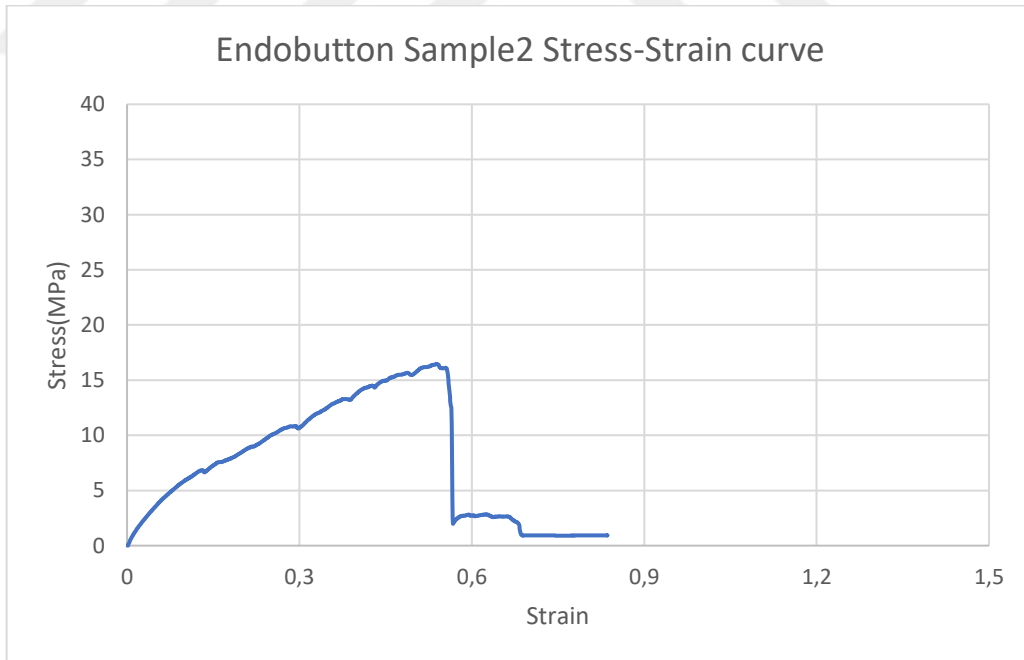


Figure 4.33 Tensile behavior characterization of Endobutton Sample2

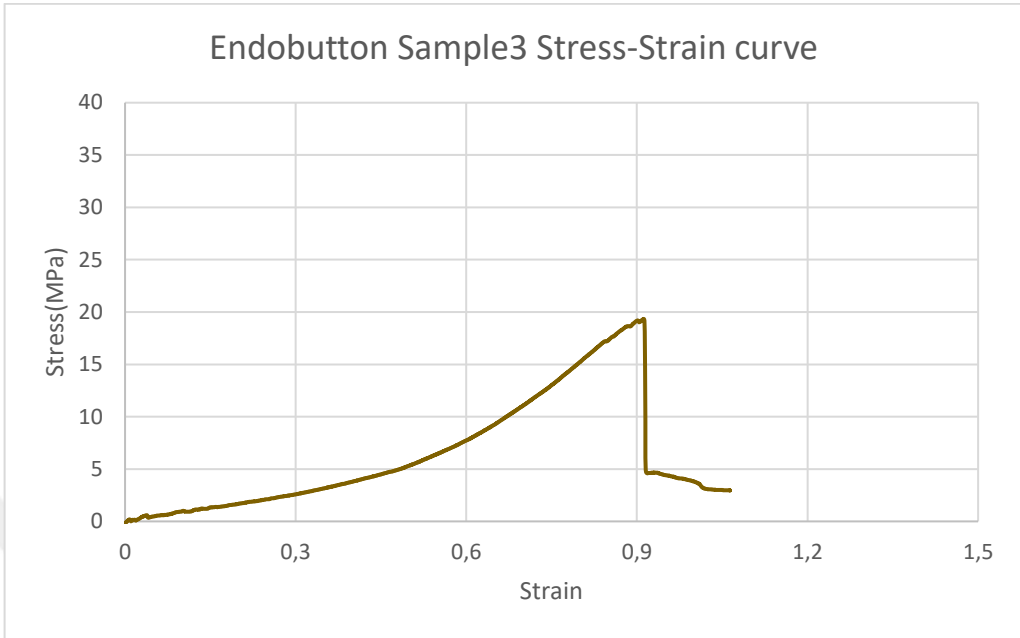


Figure 4. 34 Tensile behavior characterization of Endobutton Sample3

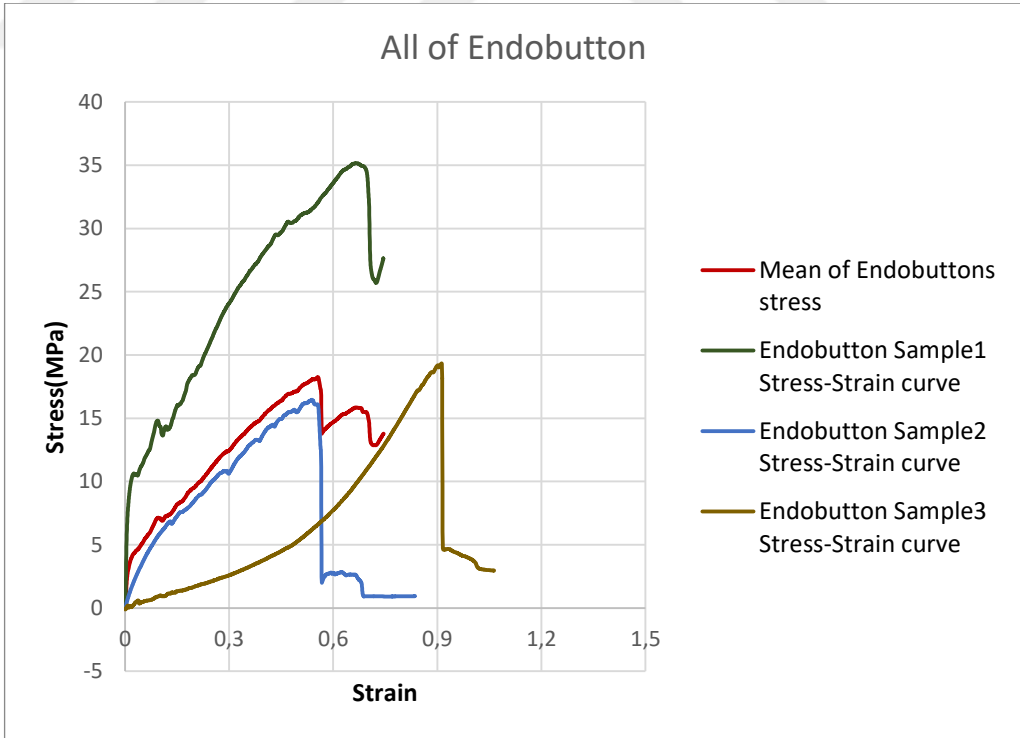


Figure 4. 35 Tensile behavior characterization of Endobutton Samples

4.3.3 Comparison of screws and Endobuttons

Mechanical properties of endobuttons and screws are evaluated with tensile test. Comparison of the mean of the samples of endobuttons and screws are given in (Figure 4.36). From (Figure 4.36 and Figure 4.37) we can see that the young modulus of Endobuttons as 26.65 MPa and screws as 28.62 MPa. Elastic modulus of the glenoid labrum is found as 26.2 ± 7.3 MPa. Since both of the fixation methods are within the range of elastic modulus of natural tissue, from Figure 4.37 it can easily be seen that fixated methods elastic modulus is within the range of natural tissue.

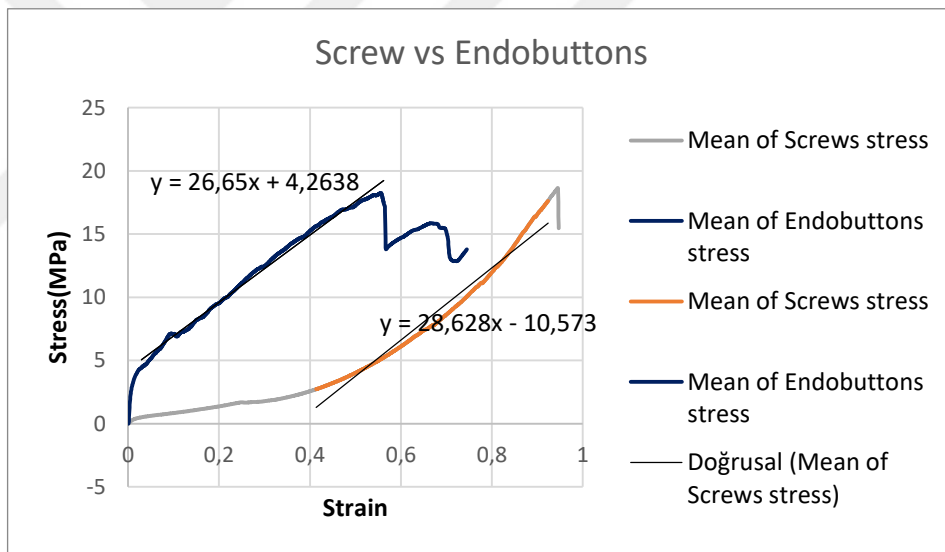


Figure 4.36 Tensile behavior characterization of Endobutton Samples and Screw Samples

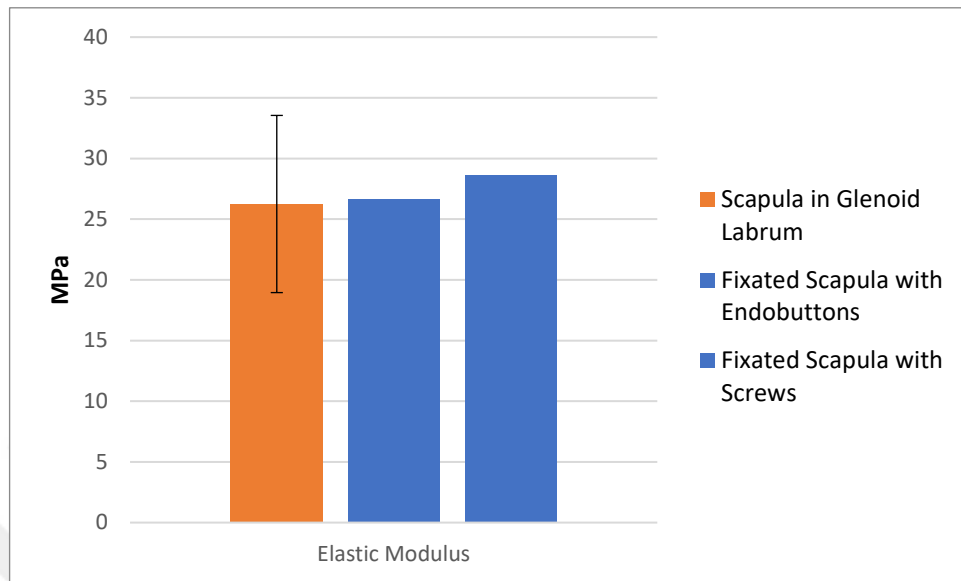


Figure 4.37 Diagram for young modulus of Endobuttons and Screws

Another comparison of these fixation methods are made with the maximum tensile stresses that samples can withstand.

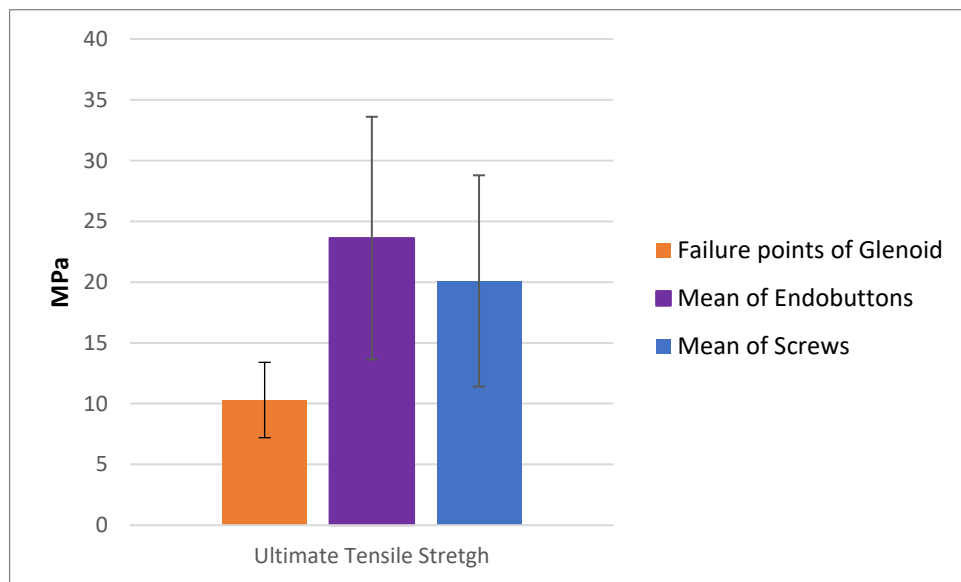


Figure 4.38 Diagram for Ultimate Tensile Stress of Endobuttons and Screws

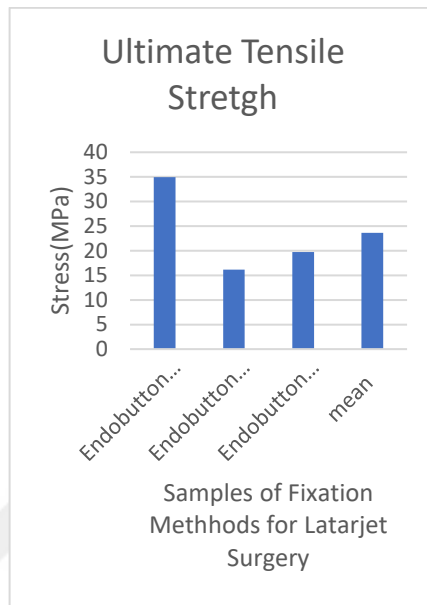


Figure 4.39 Diagram for Ultimate Tensile Stress of Endobuttons

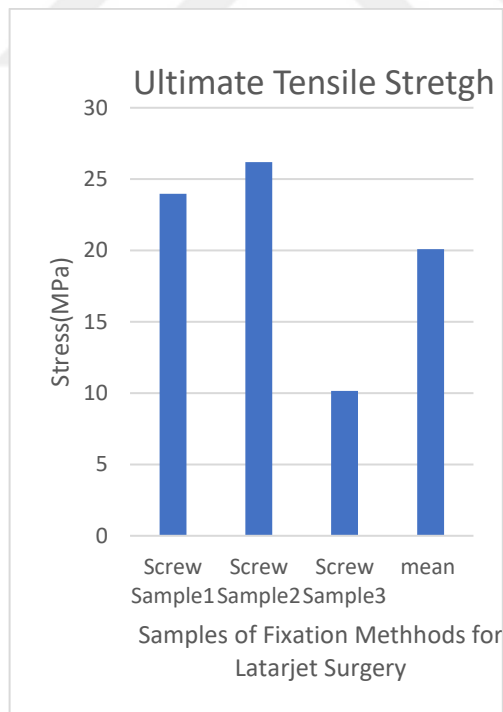


Figure 4.40 Diagram for Ultimate Tensile Stress of Screws

From (Figure 4.38), it can easily be seen that the mean of both fixation methods ultimate tensile stresses are higher than the natural tissues failure point. Moreover, the lowest point of the range of the mean of endobuttons is higher than the possible maximum of failure stress of natural tissue. Finally, the lowest point of the range of the mean of screws is equal to the possible maximum of failure stress of natural tissue.

Both the evaluation of fixation methods and natural tissue with the point of tensile strength and elastic moduli show us that both fixation methods are either equals or have mechanically higher performance than natural tissue (YARADILMIŞ, Okkaoglu et al. 2020, Huri, Hakverdiyev et al. 2021) .

4.4 Aorta Parts

4.4.1 Evaluation of aorta parts under compression stress

While we were planning to characterize the aorta mechanically, the tensile test was the first experiment that came to our mind. However, during experiments, we were not able to find appropriate holding points for the jaws of uniaxial tensile test equipment. So we plan to make a compression test. However, during the experiments, as you can see in (Figure 3.27), it was not seemed possible to standardize the force and stress related. After that, we have found a way to do the tensile test in a more standardized way.

4.4.2 Evaluation of aorta parts under tensile stress

Printing of holding helpers for jaws is made with PLA filament. With this extra equipment, we apply a uniaxial tensile test with a 10mm/min rate (Figure 3.31). A few minutes later, the elongation on the aorta part can be recognized in the (Figure 4.42). Stress-Strain curves of the samples are given in (Figures 4. 43-46). Aorta samples during the experiment are given in (Figure 4.41 and Figure 4.42)



Figure 4.41 Before the evaluation of aorta parts under tensile stress

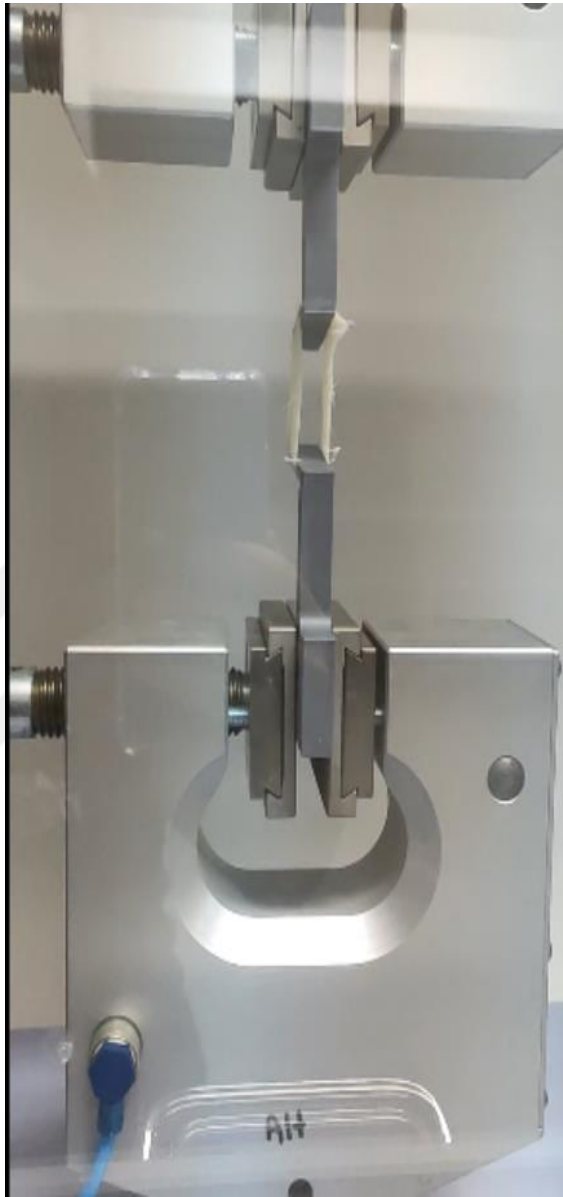


Figure 4.42 During the evaluation of aorta parts under tensile stress

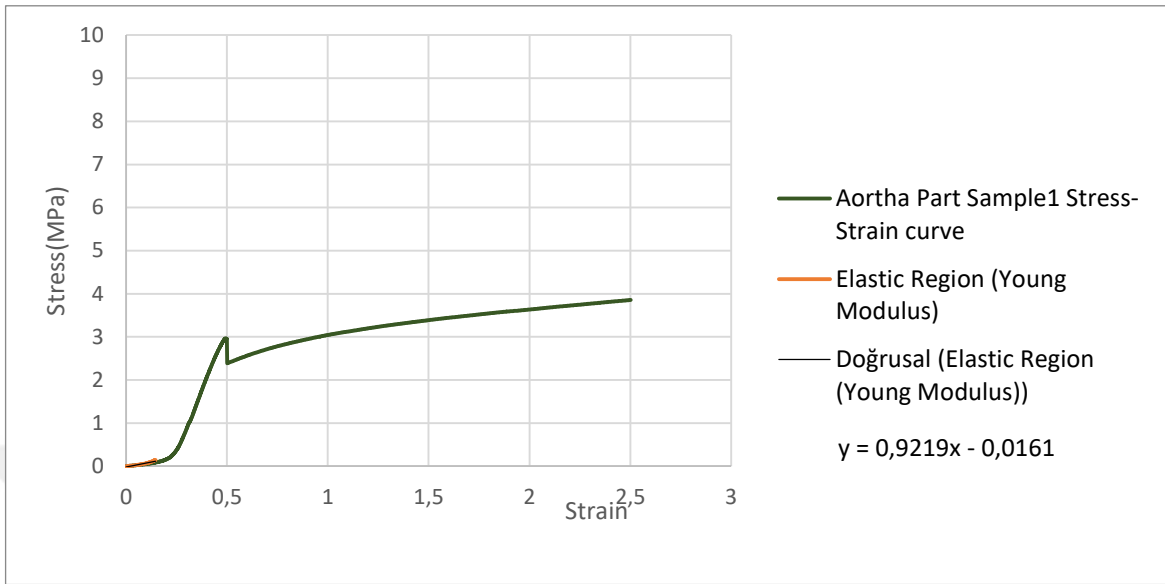


Figure 4.43 Tensile behavior characterization of Aorta Part Sample1

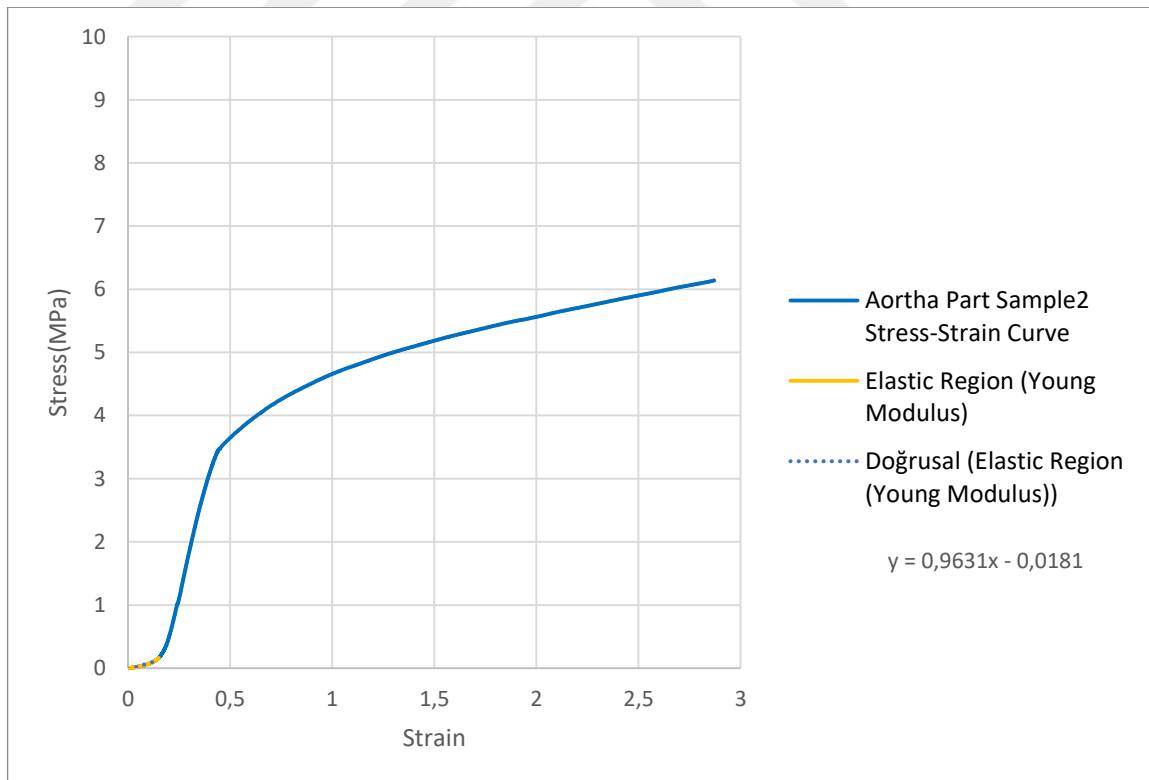


Figure 4.44 Tensile behavior characterization of Aorta Part Sample2

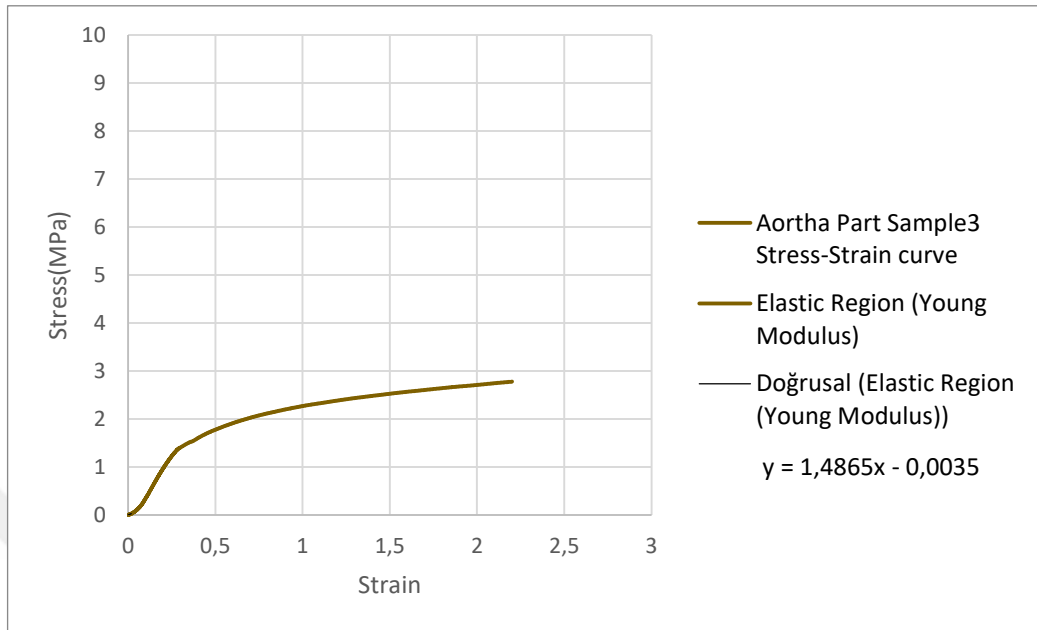


Figure 4.45 Tensile behavior characterization of Aorta Part Sample3

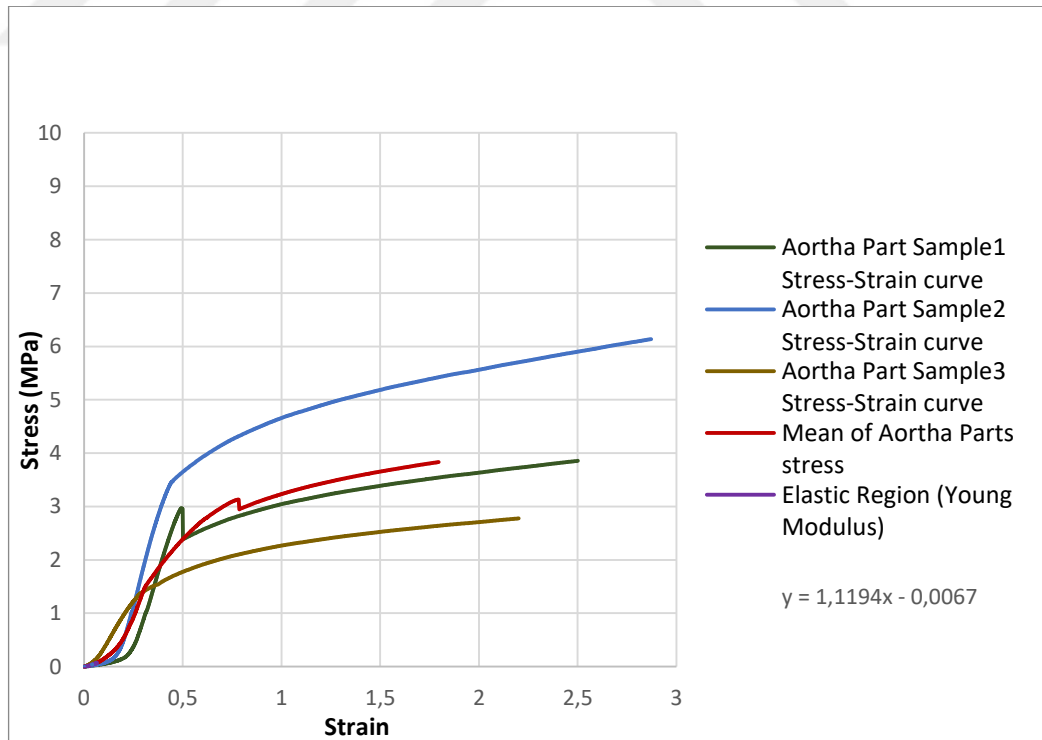


Figure 4.46 Tensile behavior characterization of Aorta Part Samples

These graphs are evaluated in terms of their young modulus and maximum elongation at break.

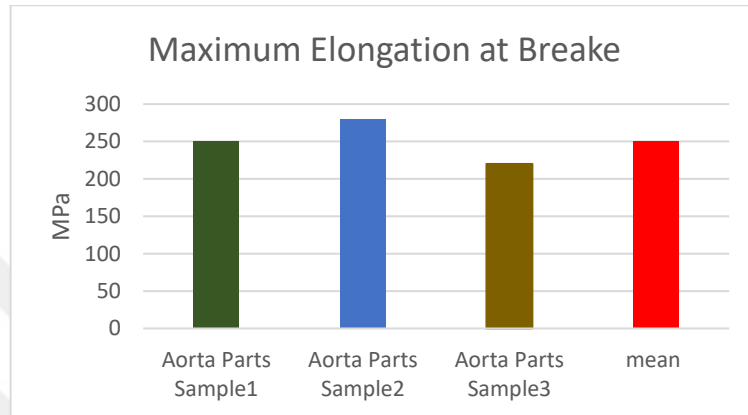


Figure 4 47 Maximum elongation of Aorta Part Samples

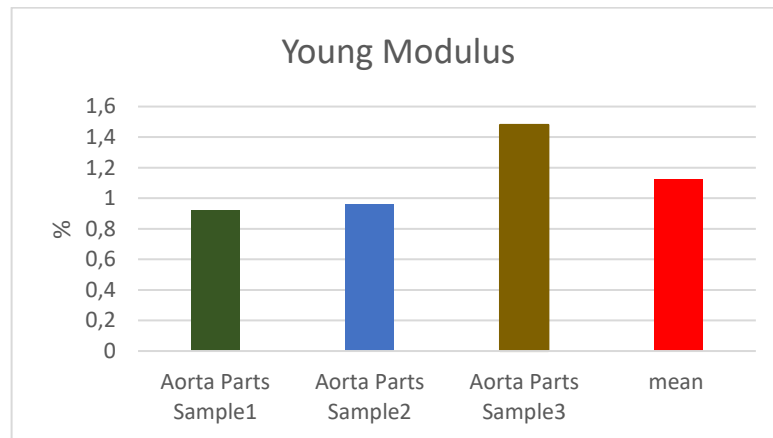


Figure 4.48 Young modulus of Aorta Part Samples

Young Modulus's of samples are similar to the tests from the literature, which are 0.95 and 1.12 ± 0.31 (Figure 4.48). Moreover, the Maximum elongation performances of samples are two times higher than the samples from the literature 95% and 250 ± 30 (Figure 4 47). We can say that these samples can be said as candidates to mimic the aorta along with these tests.

5. CONCLUSION

The Sars-Cov-2 virus started the Covid19 pandemic in eastern Asia in 2019. This infection did not have higher death ratios than the Zika virus; however, its ability to infect people and mutation made it one of the most essential pandemics of the era. Since this virus is competent in infection a mutation, it covers almost every inch of the world. This over intense situation made the world health industry insufficient for the need of the hospitals. While hospitals require too many materials, either health industries warehouses were idle, or their capacity to supply the current need was insufficient. Modern industrial methods generally require time-consuming templates or high starting budgets to establish. However, 3D printers do not require both. Since too many individuals own these devices, many people become organized and help the hospital where the health industry becomes insufficient. They simply fill in the gaps where the industry is making its preparations.

Along with this thesis, we focused on face shields for the prevention of the infection, laryngoscopes for the treatment and diagnosis of the disease. Moreover, this thesis also tried to find ways to reduce aerosol creation to protect the surgeons, who are also mentioned in this thesis as the fighter angels of the Covid 19. To reduce the aerosol creations in the surgeries, this thesis focused on two specific areas. The first one is the use of Endobuttons in the latarjet fixation surgeries instead of screws. Endobuttons is known as a reducer in the latarjet fixation surgery; hence it can be named as a less aerosol creating method. This thesis looked over the mechanic performance of Endobuttons and screws, and they found them almost similar to each other, and they can be used interchangeably in terms of mechanical properties. The other one is the creation of aorta guides for aorta stent implantation. With these guides, surgeons will be able to reduce the time of implantation during surgery since they will be doing most of the job before surgery. Due to limited time, this idea only stayed in the step of mechanical evaluation of the aorta, whether it is able or not to mimic natural tissue's mechanical properties. Further application of this idea is now discussing with several medical professionals.

Finally, this thesis discusses the ability of 3D printing to help fight against both face shields and laryngoscopes. Moreover, it looks for ideas to reduce the aerosol creation to reduce infection ways.



6. FUTURE PROSPECTS

6.1 Personal Breathing Unit

A personal breathing unit was proposed during thesis proposal. However because of the financial inadequacy it was not possible to accomplish a model. A design and fabrication of a personal breathing unit is planned if adequate financial support can be obtained.



REFERENCES

- Amato, A., et al. (2020). "Infection control in dental practice during the COVID-19 pandemic." *International journal of environmental research and public health* 17(13): 47-69.
- André, J.-C. (2017). *From Additive Manufacturing to 3D/4D Printing: Breakthrough Innovations: Programmable Material, 4D Printing and Bio-Printing*, John Wiley & Sons., 15-62.
- AO, E. C. C. (2021). "Desafios da prototipagem, confecção e utilização de videolaringoscópios produzidos por manufatura própria em impressoras 3D." *Brazilian Journal of Anesthesiology* 71(5): 5-10.
- Ayyıldız, S., et al. (2020). "3D-printed splitter for use of a single ventilator on multiple patients during COVID-19." *3D Printing and Additive Manufacturing* 7(4): 181-185.
- Boutin, S., et al. (2021). "Host factors facilitating SARS-CoV-2 virus infection and replication in the lungs." *Cellular and Molecular Life Sciences*: 1-24.
- Bowdle, A. and L. S. Munoz-Price (2020). "Preventing infection of patients and healthcare workers should be the new normal in the era of novel coronavirus epidemics." *Anesthesiology*: 4-7.
- Chavez, S., et al. (2021). "Coronavirus Disease (COVID-19): A primer for emergency physicians." *The American journal of emergency medicine* 44: 220-229.
- Chepelev, L. L. and F. J. Rybicki (2021). *The Next Pandemic and Resilience Through Strategic Manufacturing Reserves: Applying the Lessons of COVID-19 in Medical 3D Printing and Other Manufacturing*. *3D Printing in Medicine and Its Role in the COVID-19 Pandemic*, Springer: 121-127.
- Christou, A., et al. (2020). "GlasVent—The rapidly deployable emergency ventilator." *Global Challenges* 4(12): 2-46.

- dos Santos, J. R. L., et al. (2020). "Confronting COVID-19-The case of PPE and Medical Devices production using Digital Fabrication at PUC-Rio." *Strategic Design Research Journal* 13(3): 488-501.
- Edlow, B. L., et al. (2020). "Delayed reemergence of consciousness in survivors of severe COVID-19." *Neurocritical care* 33(3): 627-629.
- Ford, J., et al. (2020). "A 3D-printed nasopharyngeal swab for COVID-19 diagnostic testing." *3D printing in medicine* 6(1): 1-7.
- Gasmi, A., et al. (2020). "Individual risk management strategy and potential therapeutic options for the COVID-19 pandemic." *Clinical Immunology* 215: 108-409.
- Gereffi, G. (2020). "What does the COVID-19 pandemic teach us about global value chains? The case of medical supplies." *Journal of International Business Policy* 3(3): 287-301.
- Gökyürek, M. (2020). 3D bioprinting of parathyroid tissue. Department of Biomedical Engineering Master of Science Thesis, Graduate School of Natural and Applied Sciences, Ankara University.
- Grossin, D., et al. (2021). "A review of additive manufacturing of ceramics by powder bed selective laser processing (sintering/melting): Calcium phosphate, silicon carbide, zirconia, alumina, and their composites." *Open Ceramics*: 100-173.
- Guvener, O., et al. (2021). "Novel additive manufacturing applications for communicable disease prevention and control: focus on recent COVID-19 pandemic." *Emergent materials*: 1-11.
- Hull, C. (2012). "On stereolithography." *Virtual and Physical Prototyping* 7(3): 176-177.
- Huri, G., et al. (2021). "Biomechanical Strength of Screw Versus Suture Button Fixation in the Latarjet Procedure: A Cadaver Study." *Journal of Shoulder and Elbow Surgery* 30(7): e449.
- Iuliano, L., et al. (2019). "Characterization of Inconel 718 fabricated by Selective Laser Melting (SLM) to achieve more productive parameters." 2-6.

- Juwarkar, C. S. (2013). "Cleaning and sterilisation of anaesthetic equipment." *Indian Journal of Anaesthesia* 57(5): 541.
- Kamran, M. and A. Saxena (2016). "A comprehensive study on 3D printing technology." *MIT Int J Mech Eng* 6(2): 63-69.
- Lasprilla, A. J., et al. (2012). "Poly-lactic acid synthesis for application in biomedical devices—A review." *Biotechnology advances* 30(1): 321-328.
- Liao, M., et al. (2021). "A technical review of face mask wearing in preventing respiratory COVID-19 transmission." *Current Opinion in Colloid & Interface Science*: 101-417.
- Lu, D., et al. (2016). "A comparison of double Endobutton and triple Endobutton techniques for acute acromioclavicular joint dislocation." *Orthopaedics & Traumatology: Surgery & Research* 102(7): 891-895.
- Machan, M. D. (2012). "Infection control practices of laryngoscope blades: A review of the literature." *AANA J* 80(4): 274-278.
- Meglioli, M., et al. (2020). "3D printing workflows for printing individualized personal protective equipment: an overview." *Transactions on Additive Manufacturing Meets Medicine* 2(1): 3-11.
- Mlcak, R. P., et al. (2007). "Respiratory management of inhalation injury." *burns* 33(1): 2-13.
- O'Dowd, K., et al. (2020). "Face masks and respirators in the fight against the COVID-19 pandemic: A review of current materials, advances and future perspectives." *Materials* 13(15): 33-63.
- Oosthuizen, G. A., et al. (2013). "Evaluation of rapid product development technologies for production of prosthesis in developing communities." *Proceedings of SAIEE* 25: 4-7.
- Pastia, C. (2021). *3D Printing of Buildings. Limits, Design, Advantages and Disadvantages. Could This Technique Contribute to Sustainability of Future Buildings? Critical Thinking in the Sustainable Rehabilitation and Risk Management of the Built*

Environment: CRIT-RE-BUILT. Proceedings of the International Conference, Iași, Romania, November 7-9, 2019, Springer Nature, 2-98.

Ranney, M. L., et al. (2020). "Critical supply shortages—the need for ventilators and personal protective equipment during the Covid-19 pandemic." *New England Journal of Medicine* 382(18): 10-41.

Rendeki, S., et al. (2020). "An overview on personal protective equipment (PPE) fabricated with additive manufacturing technologies in the era of COVID-19 pandemic." *Polymers* 12(11): 2703.

Şahada, A., et al. "Role of Biomedical Engineering during COVID-19 Pandemic." *Natural and Applied Sciences Journal* 3(1): 1-16.

Singh, R. and N. Ranjan (2018). "Experimental investigations for preparation of biocompatible feedstock filament of fused deposition modeling (FDM) using twin screw extrusion process." *Journal of Thermoplastic Composite Materials* 31(11): 1455-1469.

Somashekhar, S., et al. (2020). ASI's consensus guidelines: ABCs of what to do and what not during the COVID-19 pandemic, 3-5, Springer.

Su, A. and S. J. Al'Aref (2018). History of 3D printing. *3D Printing Applications in Cardiovascular Medicine*, Elsevier: 1-10.

Tu, J., et al. (2012). *Computational fluid and particle dynamics in the human respiratory system*, Springer Science & Business Media.

weball3dp (2021). from <https://all3dp.com/2/stereolithography-3d-printing-simply-explained/>, Retrieved 10 May 2021.

webotonomfabrika (2021). Retrieved 08 April 2021, from <https://www.otonomfabrika.com/katmanli-imalat-uretim-nedir/>, Retrieved 08 April 2021.

Wohlers, T. and T. Gornet (2014). "History of additive manufacturing." *Wohlers report* 24(2014): 1-18.

Yao, W., et al. (2020). "Emergency tracheal intubation in 202 patients with COVID-19 in Wuhan, China: lessons learnt and international expert recommendations." *British journal of anaesthesia* 125(1): e28-e37.

YARADILMIŞ, Y. U., et al. (2020). "Femur boyun kırıklarında kırık lokalizasyonunun instabilite ile ilişkisi: Biyomekanik çalışma." *Ege Tıp Dergisi* 59(3): 160-164.

Yeong, W. Y. and C. K. Chua (2014). *Bioprinting: principles and applications*, World Scientific Publishing Co Inc., 6-8.

